Komatiitic and Iron-rich Tholeiitic Lavas of Munro Township, Northeast Ontario

by N. T. ARNDT,[1]* A. J. NALDRETT,[1] and D. R. PYKE[2]

[1] Dept. of Geology, University of Toronto, Toronto, Canada, M5S 1A1
[2] Division of Mines, Ministry of Natural Resources, Queen's Park, Toronto, Canada

(Received 8 March 1976; in revised form 6 October 1976)

ABSTRACT

Munro Township, in the Archean Abitibi greenstone belt of northeast Ontario, contains volcanic and hypabyssal rocks of two magma series: (1) an Fe-rich tholeiitic series of basaltic to dacitic lava flows (3–10 m thick), layered peridotite–pyroxenite–gabbro flows (120 m thick), and layered sills (700 m thick); (2) an ultramafic–mafic komatiitic series, comprising discrete lava flows of peridotitic to andesitic composition (1–17 m thick), layered peridotite–gabbro flows (120 m thick), and layered sills (500 m thick). The komatiitic lavas form a succession about 1000 m thick that is both underlain and overlain by thicker successions of tholeiitic volcanic rocks.

Three types of komatiite are recognized: peridotitic, pyroxenitic, and basaltic komatiites. The most ultramafic are peridotitic cumulates rich in forsteritic olivine (Fo_{89-94}), at the bases of flows and sills. Many less mafic peridotitic komatiites (MgO: 20–30 per cent), which typically form the upper parts of flows and the marginal parts of small intrusions, exhibit spinifex textures indicative of their formation from ultrabasic liquids. Pyroxenitic komatiites (MgO: 12–20 per cent) also may contain olivine, but are dominated by clinopyroxene, usually in spinifex textures. Basaltic komatiites (MgO $<$ 12 per cent) are composed mainly of clinopyroxene and plagioclase or devitrified glass, rarely in spinifex texture and more commonly in equigranular textures. Peridotitic komatiite with roughly 30 per cent MgO appears to represent a parental liquid from which the more ultramafic komatiites formed by accumulation of olivine, and the less mafic types were derived by fractionation of olivine, joined and finally succeeded in later stages by clinopyroxene and plagioclase.

Komatiites of Munro Township share many of the characteristics of the komatiites from the Barberton Mountain Land, South Africa (Voljoen & Viljoen, 1969*a* and *b*), but lack the high CaO/Al_2O_3 ratios that distinguish the Barberton rocks. The Munro komatiites are identical in this respect to ultramafic volcanic rocks in Australia, Canada, Rhodesia, and India. It is proposed that the definition of the term komatiite be broadened so that it includes all members of this ultramafic–mafic rock series, not only those from Barberton Mountain Land. The proposed criteria are: (1) highly ultramafic compositions in noncumulate lavas; (2) unusual volcanic structures such as spinifex texture and polyhedral jointing; (3) low Fe/Mg ratios at given Al_2O_3 values or high CaO/Al_2O_3 ratios; low TiO_2 at given SiO_2; and high MgO, NiO, and Cr_2O_3.

INTRODUCTION

THIS paper is the product of a comprehensive investigation of Archean ultramafic lavas and related rocks in Munro Township, northeast Ontario, and follows an initial study by Pyke, Naldrett & Eckstrand (1973) of a large outcrop of ultramafic lava flows in the center of the township. The primary aim of this

* Present Address: *Geophysical Laboratory, Carnegie Institution of Washington, 2801 Upton St., N.W., Washington D.C. 20008, U.S.A.*

[Journal of Petrology, Vol. 18, Part 2, pp. 319–369, 1977]

Downloaded from https://academic.oup.com/petrology/article-abstract/18/2/319/1565696 by University of California, San Diego Library user on 28 March 2019

study was to document further the unusual ultramafic lavas and to investigate their relationship to mafic volcanic and ultramafic cumulate rocks in the area.

Definition of komatiite

The term komatiite was introduced by Viljoen & Viljoen (1969*a*) for peridotitic and related mafic lavas of the Barberton Mountain Land of South Africa. They stated that the Barberton komatiites were distinguishable from more

TABLE 1

Classification of komatiites in Munro Township

	Field characteristics	*Petrologic characteristics*	MgO*
Peridotitic komatiite	The most magnesian types (MgO > 30%) are massive dark gray to black, olivine-rich rocks, devoid of conspicuous volcanic features, and form the basal cumulate sections of spinifex-bearing flows, or the central parts of intrusions. Less magnesian types are paler gray-green rocks weathering chocolate-brown; they occur in the spinifex-textured sections of zoned flows, or in spinifex-free flows, or in the marginal parts of small intrusions. Spinifex-free lava is characterized by polyhedral jointing.	All types are composed of olivine grains and minor chrome spinel in a matrix of fine-grained clinopyroxene and devitrified glass. In cumulates olivine grains are close-packed, solid, roughly equant and comprise 60 to 80% of the rock; in spinifex texture olivine forms large skeletal platy grains (35 to 60%); and in spinifex-free, non-cumulate rock, olivine may be equant or skeletal (45 to 70%).	MgO > 20%
Pyroxenitic komatiite	Forms low, flat outcrops of soft, gray-green, crumbly lava that breaks with a hackly fracture; it may contain clinopyroxene spinifex, polyhedral jointing, lava toes or varioles.	Equant solid, or platy skeletal grains of olivine (0 to 35%) in fine-grained matrix of clinopyroxene and devitrified glass; or skeletal subcalcic clinopyroxene needles in devitrified glass groundmass; or closely-packed equant grains of pyroxene and olivine. No plagioclase.	MgO between 12 and 20%
Basaltic komatiite	Forms massive outcrops of hard pale-gray-green lava, and may contain lava toes and hyaloclastite flowtops, or may be massive. Rare examples are clinopyroxene spinifex-textured.	No olivine in the groundmass; plagioclase instead. Clinopyroxene and plagioclase form spinifex texture, 'graphic' intergrowths, or normal subophitic texture.	MgO < 12%

* Anhydrous values.

familiar ultramafic rocks by textural features indicative of extrusive origin as mobile lavas, and by chemical features such as high SiO_2, high Fe/Mg, low alkali elements, and, especially, high CaO/Al_2O_3. Brooks & Hart (1974) quantified these characteristics and suggested that komatiites were noncumulate rocks with MgO < 9 per cent, K_2O < 0·5 per cent, TiO_2 < 0·9 per cent, and $CaO/Al_2O_3 > 1$.

Downloaded from https://academic.oup.com/petrology/article-abstract/18/2/319/1565696 by University of California, San Diego Library user on 28 March 2019

Ultramafic lavas in Munro Township and in many other areas, *e.g.* Australia (Williams, 1972), India (Viswanathan, 1974), Rhodesia (Bickle *et al.*, 1975) share most of the characteristics of the Barberton komatiites but lack their high CaO/Al_2O_3 ratios. The average CaO/Al_2O_3 of Munro komatiites is 0·84, and over half the analysed samples have ratios less than 1. Because the Brooks & Hart (1974) definition applies to only a small proportion of the rocks from Munro Township and the other areas mentioned, a new definition of komatiite is proposed that includes a wider range of ultramafic–mafic volcanic and hypabyssal rocks. In later sections we describe field, petrologic, and chemical criteria, developed for Munro, that form the basis of the re-definition, and we present data from other areas to show that the Munro rocks are representative of the series as a whole.

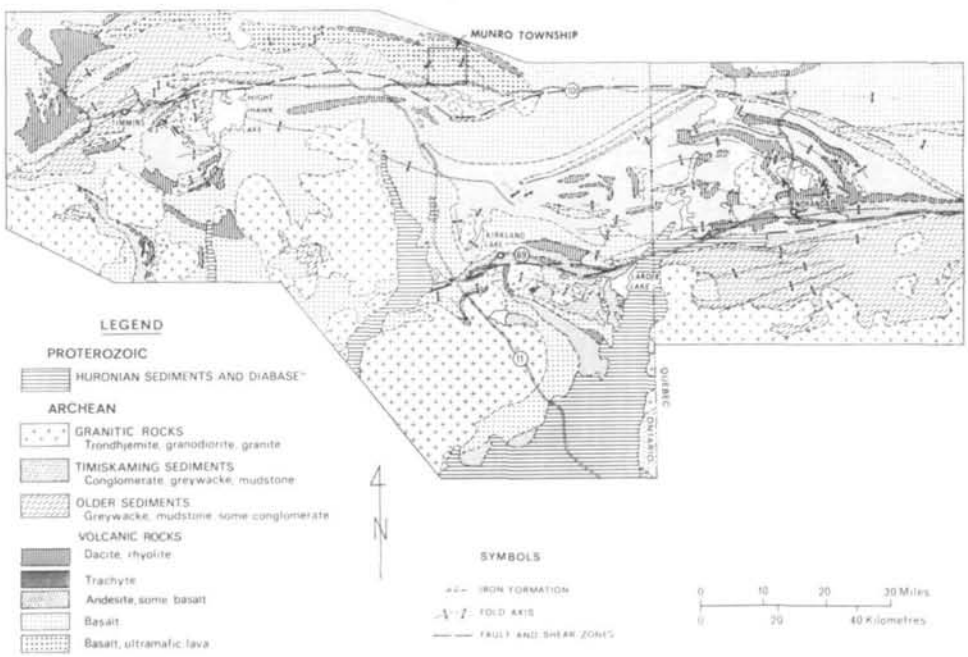

FIG. 1. Map showing the locations of Munro Township and geology of the surrounding area (after Goodwin, 1976).

Classification of Munro komatiites

Three types of komatiites are recognized: peridotitic, pyroxenitic, and basaltic komatiites. The field, petrologic, and chemical criteria for the subdivision, and brief descriptions of each type are given in Table 1.

Geological setting

Munro Township is situated in northeast Ontario, 50 km north of the town of Kirkland Lake (Fig. 1), and lies within the 2·7 b.y. old Abitibi greenstone belt

Downloaded from https://academic.oup.com/petrology/article-abstract/18/2/319/1565696 by University of California, San Diego Library user on 28 March 2019

in the Superior Province of the Canadian Shield. The township and adjoining areas were originally mapped by Satterly (1949, 1951, 1952) and Satterly & Armstrong (1947). The Abitibi belt has been studied by Goodwin (1968, 1973), Goodwin & Ridler (1969), Jolly (1974), 1975), and Pyke & Jensen (1976), and rocks in the area have been dated by Krogh & Davis (1971). Brief reviews of the geology are found in MacRae (1969) and Pyke *et al.* (1973).

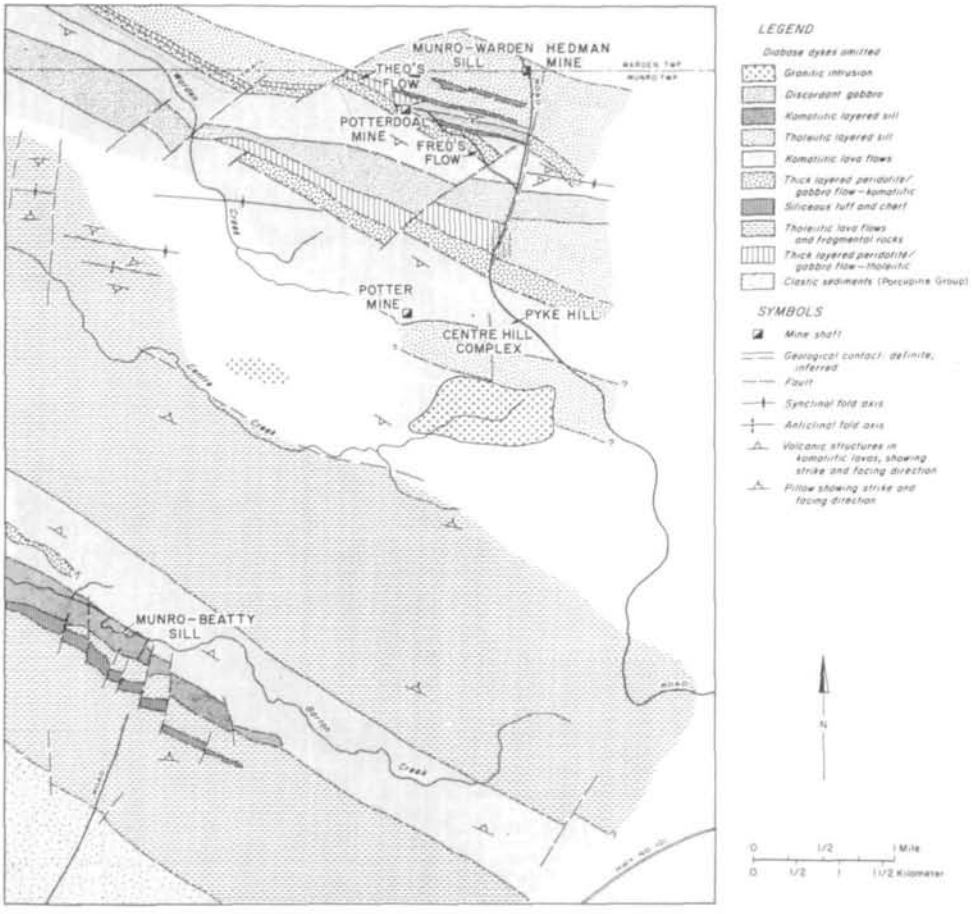

FIG. 2. Geology of Munro Township (modified from Satterly, 1951).

The predominant rocks in Munro Township (Figs. 2 and 3) are komatiitic ultramafic and mafic lavas, and tholeiitic volcanic rocks. Most abundant are thin (2 m to 20 m thick) pillowed and massive flows with relatively uniform compositions, which are interlayered with much thicker (100 m to 300 m thick) flows that are differentiated from peridotite at the base to gabbro near the top. The volcanic rocks are intercalated with thin, but persistent, bands of siliceous tuff and chert, and are intruded by (a) small peridotite sills and dikes, (b) large

Downloaded from https://academic.oup.com/petrology/article-abstract/18/2/319/1565696 by University of California, San Diego Library user on 28 March 2019

layered peridotite–gabbro sills, (c) large discordant gabbroic intrusions, and (d) much younger (Proterozoic) diabase dikes.

All rocks except the discordant gabbros and diabase dikes are folded and disrupted by faulting. A major east-southeast fault in the northern part of the township has repeated much of the volcanic sequence. Metamorphic grade in the intensively studied parts of the township is prehnite–pumpellyite facies.

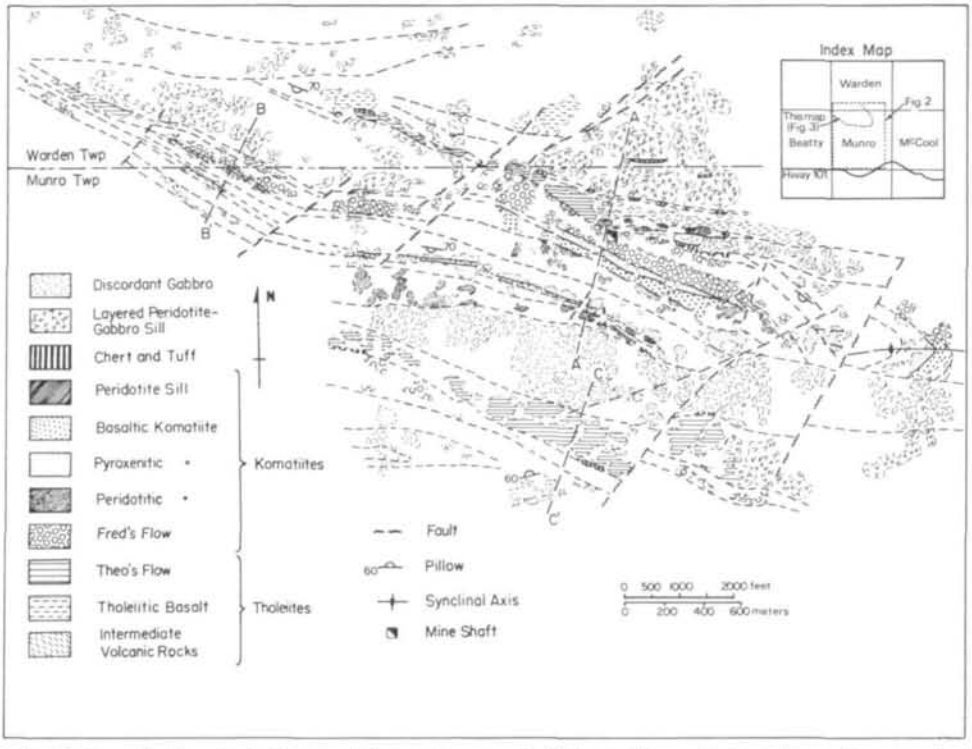

FIG. 3. Simplified geological map of the northern part of Munro Township and the southern part of Warden Township. Diabase dykes omitted.

Stratigraphy

Figure 4 shows three generalized stratigraphic sections through the volcanic pile in northern Munro Township. The central section illustrates the thickest and most complete part of the pile; the section to the west demonstrates thinning of most units and increasing abundance of mafic komatiites in that direction; and the southern section contains the same units repeated by the major east-southeast fault.

The thick basal section of basaltic and andesitic tholeiitic lava flows and fragmental rocks is overlain by komatiites of peridotitic to basaltic composition. In the southern part of the township a second sequence of tholeiites overlies the komatiites. Although a few komatiites of andesitic composition are interlayered with the upper tholeiites in the north of the township, generally there is little

Downloaded from https://academic.oup.com/petrology/article-abstract/18/2/319/1565696 by University of California, San Diego Library user on 28 March 2019

interlayering of the two lava types. A thick, layered peridotite–gabbro flow of the tholeiitic series (referred to as Theo's Flow) terminates the tholeiitic succession and a similar thick, layered flow of the komatiitic series (Fred's Flow) forms the base of the komatiitic succession. Thick, complexly-layered sills, the Munro–Warden Complex and the Beatty Sill (MacRae, 1969), intrude at the

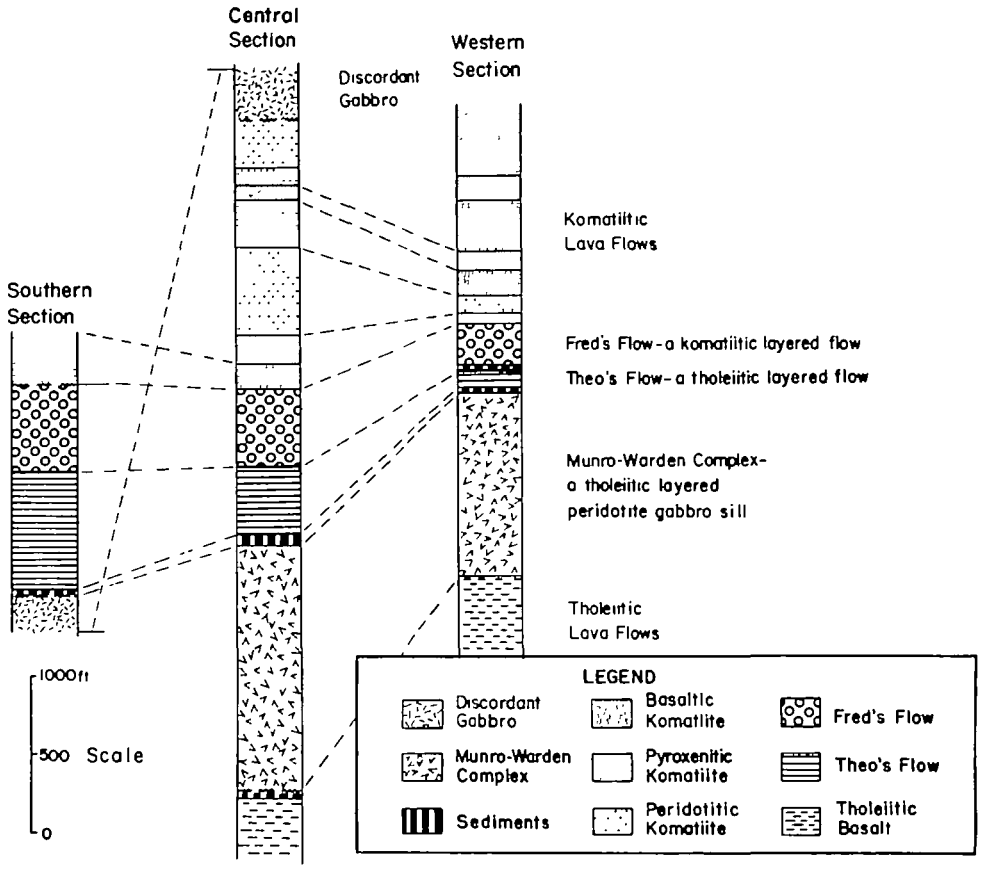

FIG. 4. Three stragigraphic sections of the volcanic succession in the northern part of Munro Township. Section locations are shown in Fig. 3. The komatiitic succession is about 800 m thick.

interface between the two successions. The ultramafic lava flows of the outcrop studied by Pyke *et al.* (1973) (called 'Pyke Hill' in this paper) are correlated with the lowermost ultramafic lavas in the succession shown in Figs. 4 and 5.

Cyclic variation in the compositions of komatiitic lavas is illustrated in Fig. 5. The lower two cycles start with relatively thin (1 to 3 m) ultramafic flows, some of which are spinifex-textured,[1] and end with thicker (3 to 20 m thick) massive

[1] Spinifex, a texture characteristic of ultramafic and mafic komatiitic lavas, has been described by Nesbitt (1971), Pyke *et al.* (1973), and Donaldson (1974). In this paper the term is applied to textures in which large plates, needles or complex skeletal grains of olivine or clinopyroxene are oriented randomly or parallel to one another in matrices of fine skeletal grains of clinopyroxene, and devitrified glass.

Downloaded from https://academic.oup.com/petrology/article-abstract/18/2/319/1565696 by University of California, San Diego Library user on 28 March 2019

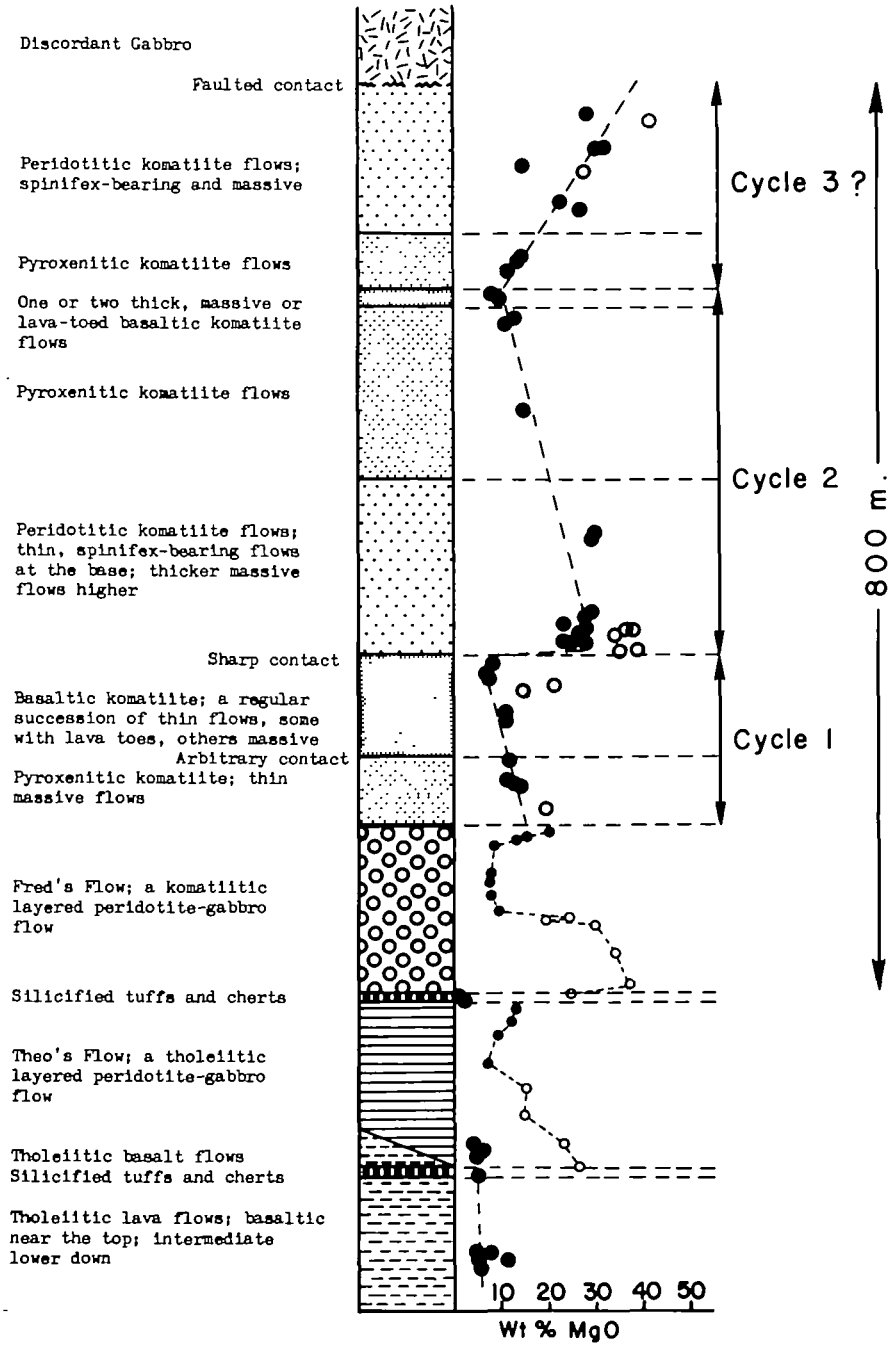

FIG. 5. Detailed, but generalized section through the Munro volcanic pile showing MgO variations in the lavas. Legend as in Fig. 4. *Closed circles* denote rocks representing magmatic liquids, *open circles* cumulate rocks.

Downloaded from https://academic.oup.com/petrology/article-abstract/18/2/319/1565696 by University of California, San Diego Library user on 28 March 2019

mafic flows. In the lower part of what may be a third cycle truncated by a gabbro intrusion, the composition of lava flows becomes more mafic with increasing stratigraphic height.

In the center of the volcanic pile (Fig. 3) peridotitic komatiites form about 45 per cent of the total section (see Table 1), pyroxenitic komatiites form about 35 per cent and basaltic komatiites about 20 per cent. To the west the proportion of pyroxenitic and basaltic komatiites is higher. In all sections pyroxenitic komatiites with 15 to 20 per cent MgO are much less common than other types.

PERIDOTITIC KOMATIITES

Description of flows

Rocks of this type are best exposed, and have been studied most intensively at Pyke Hill (Fig. 6). In their study, Pyke *et al.* (1973) concentrated primarily on flows with thick spinifex-textured upper portions and massive lower portions. This type of flow is now considered as an end-member of a continuum that ranges through flows with very thin spinifex-textured zones, to flows devoid of spinifex texture. Examples of three flows in this continuum are illustrated in Fig. 7. All types range in thickness from 50 cm to 17 m, and in length from 5 m to at least 200 m. Flows devoid of spinifex texture tend to be thicker, but shorter than flows with spinifex texture.

The type of flow with a thick spinifex-textured zone (Flow A, Fig. 7) has a chilled, aphanitic cap-rock, containing a few solid, equant olivine phenocrysts and more common very fine-grained, randomly-oriented, equant skeletal or thin-bladed olivine crystals set in a matrix of glass now altered to chlorite and serpentine (Plate 1A). Amygdules filled with pale green, microcrystalline quartz, or filled, partially or completely, with former glass may be present. The cap-rock is cut by jointing that breaks it into polyhedra 3 to 20 cm in maximum dimensions, producing a structure that superficially resembles a breccia, but that differs from a true rubble breccia in that the polyhedra are not displaced with respect to one another. True breccias are not well developed at Pyke Hill, but in the Alexo area, 60 km west of Munro Township, zones of ultramafic rubble overlie peridotitic komatiite flows.

The bladed olivine crystals increase in size downwards from aphanitic cap-rock into the spinifex-textured portion of the flow (Plate 1B). The orientation of olivine blades in the upper part of the spinifex zone is random. In the lower part the blades are arranged parallel to one another in books or sheaths that are oriented subperpendicular to the plane of the flow. Pyke *et al.* (1973) refer to the upper, polyhedrally-jointed cap-rock as the A_1 zone and the underlying, coarser grained spinifex-textured material as the A_2 zone. In general, the size of the olivine blades progressively increases downwards in the spinifex zone, but reversals do occur. Figure 8 shows the variation in the average width of spinifex blades across the A_1 and A_2 zones of a flow.

Downloaded from https://academic.oup.com/petrology/article-abstract/18/2/319/1565696 by University of California, San Diego Library user on 28 March 2019

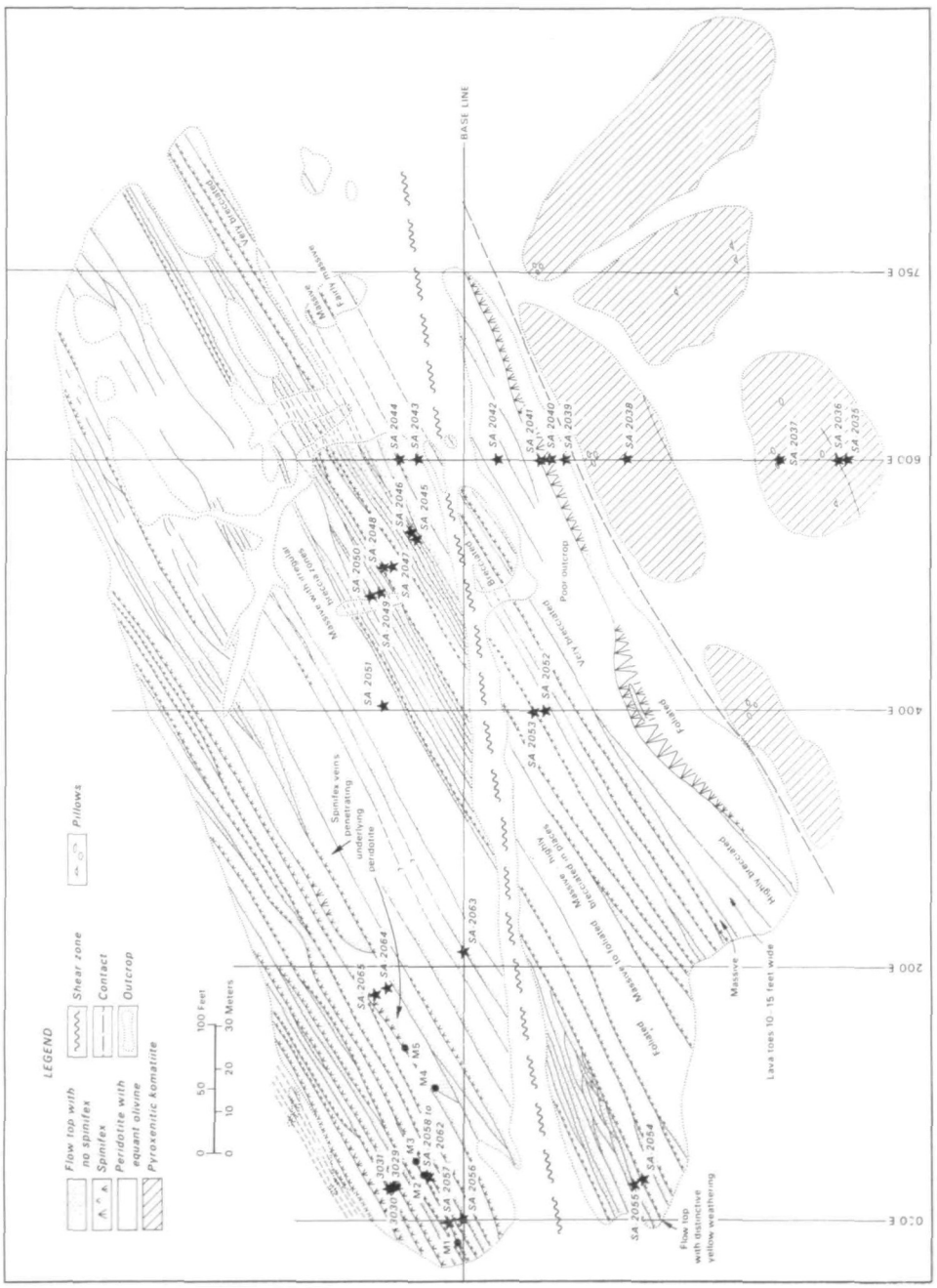

FIG. 6. Geological map of Pyke Hill, showing peridotitic komatiite lava flows, hand sample locations (*stars*), and drill hole locations (M1 to M4). (Modified from Pyke *et al.* 1973.)

Downloaded from https://academic.oup.com/petrology/article-abstract/18/2/319/1565696 by University of California, San Diego Library user on 28 March 2019

The A_2 zone is in sharp contact with the underlying B_1 zone, which consists of tabular olivine grains of a more obviously skeletal habit than those of the A_2 zone, oriented parallel to the plane of the flow. The B_1 zone has a maximum thickness of about 30 cm, but may change rapidly along strike and is sometimes absent. The elongate, hollow, skeletal needles of the B_1 zone give way downwards

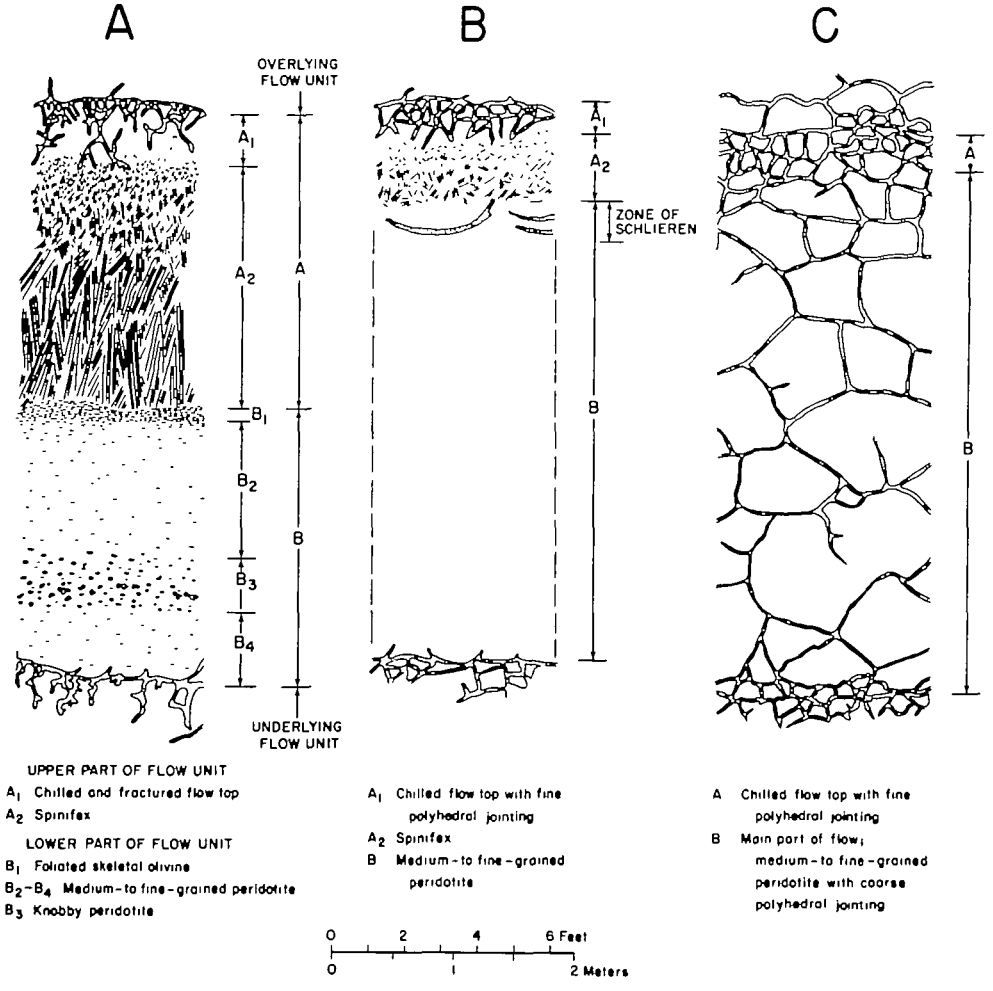

FIG. 7. Diagrammatic sections through three types of peridotitic lava flows: A, a flow with an upper spinifex zone; B, a flow with limited spinifex texture; C, a flow without spinifex texture.

to solid, more equant grains of the B_2 zone (Plate 1C). The equant grains are similar to cumulus olivine crystals in peridotites from many environments but are set in a matrix of skeletal subcalcic clinopyroxene, cruciform, dendritic or euhedral chromite, and hydrous alteration after glass. Highly elongate, partially skeletal olivine grains also are present in minor amounts. The long dimensions of these grains define a rough foliation parallel to the plane of the flow. A progres-

Downloaded from https://academic.oup.com/petrology/article-abstract/18/2/319/1565696 by University of California, San Diego Library user on 28 March 2019

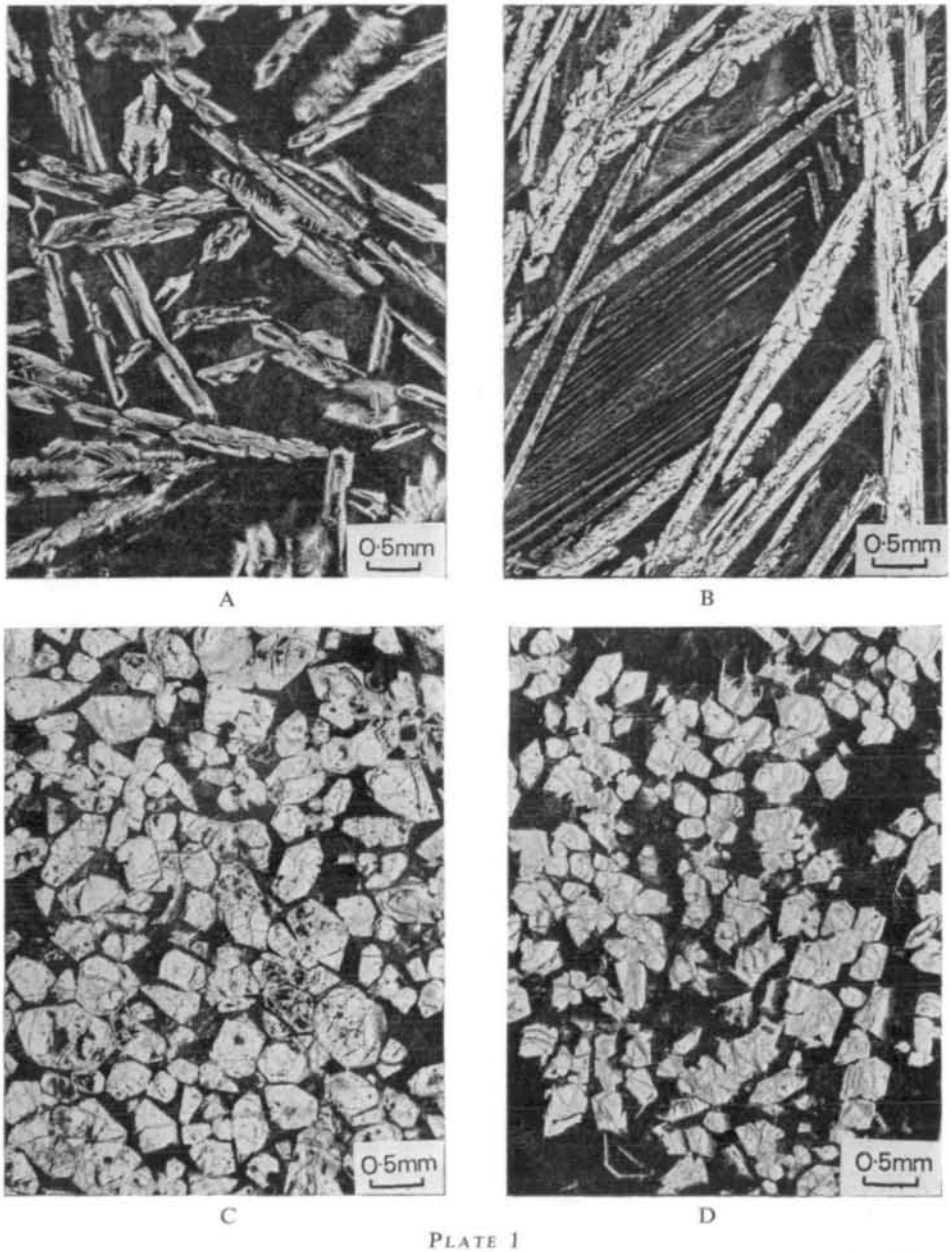

PLATE 1

PLATE 1A. Photomicrograph of the flow top of a spinifex-textured peridotitic komatiite flow. Skeletal grains of olivine (serpentinized) set in a fine grained devitrified glass matrix.

PLATE 1B. Photomicrograph of the upper part of the spinifex-textured zone of a peridotitic komatiite flow. Skeletal plates of olivine (serpentinized) are randomly oriented in a matrix of clinopyroxene and devitrified glass.

PLATE 1C. Photomicrograph of cumulate peridotitic komatiite of the B zone of a spinifex-textured flow. Equant, solid olivine grains (serpentinized) within a matrix of clinopyroxene and devitrified glass.

PLATE 1D. Photomicrograph of spinifex-free peridotitic komatiite lava. Grains of olivine, which are essentially solid but with skeletal overgrowths, are set within a matrix of clinopyroxene and devitrified glass.

Downloaded from https://academic.oup.com/petrology/article-abstract/18/2/319/1565696 by University of California, San Diego Library user on 28 March 2019

A B

PLATE 2

PLATE 2A. Relatively small polyhedra at the top of a spinifex-free peridotitic komatiite flow.
PLATE 2B. Crescent-shaped fractures filled with spinifex-textured peridotitic komatiite in the upper part of a peridotitic komatiite flow with limited development of spinifex texture.

sive downward decrease in grainsize (Fig. 8) is characteristic of olivine of the B zone.

Pyke *et al.* (1973) describe a zone referred to as 'knobby peridotite' (B_3 zone) featuring a rough weathered surface due to the presence of rounded accumulations of matrix material. Although common in the flows of Pyke Hill, this type of peridotite is rarely present further north in the township.

More than half the flows exposed at Pyke Hill have no spinifex texture and are of the type shown on the right in Fig. 7 (Flow C). These flows are pervaded by polyhedral jointing like that in the cap-rock (A_1 zone) of spinifex-textured flows. The joints are close-spaced and distinctly rectangular or polyhedral near the tops of the flows (Plate 2A) and are longer, thicker, more widely spaced, and gently curved in the centers of flows. The lava in this type of flow consists of 45–55 per cent equant olivine crystals that commonly have overgrowths of skeletal olivine (Plate 1D). Although the proportion of olivine is much lower than in the B zones of spinifex-textured flows, the size and habit of the olivine grains is similar. The matrix consists of chlorite altered from glass and skeletal, dendritic, radiating and plumose sprays of clinopyroxene. Chromite forms cruciform and dendritic crystals, and less commonly, equant, cube-shaped grains.

In typical examples of the type of flow with limited spinifex texture (Fig. 7B), a polyhedrally-jointed A_1 zone is underlain by a thin (ca. 1 m) spinifex-textured A_2 zone. Both these zones are similar to their counterparts in the first type of

Downloaded from https://academic.oup.com/petrology/article-abstract/18/2/319/1565696 by University of California, San Diego Library user on 28 March 2019

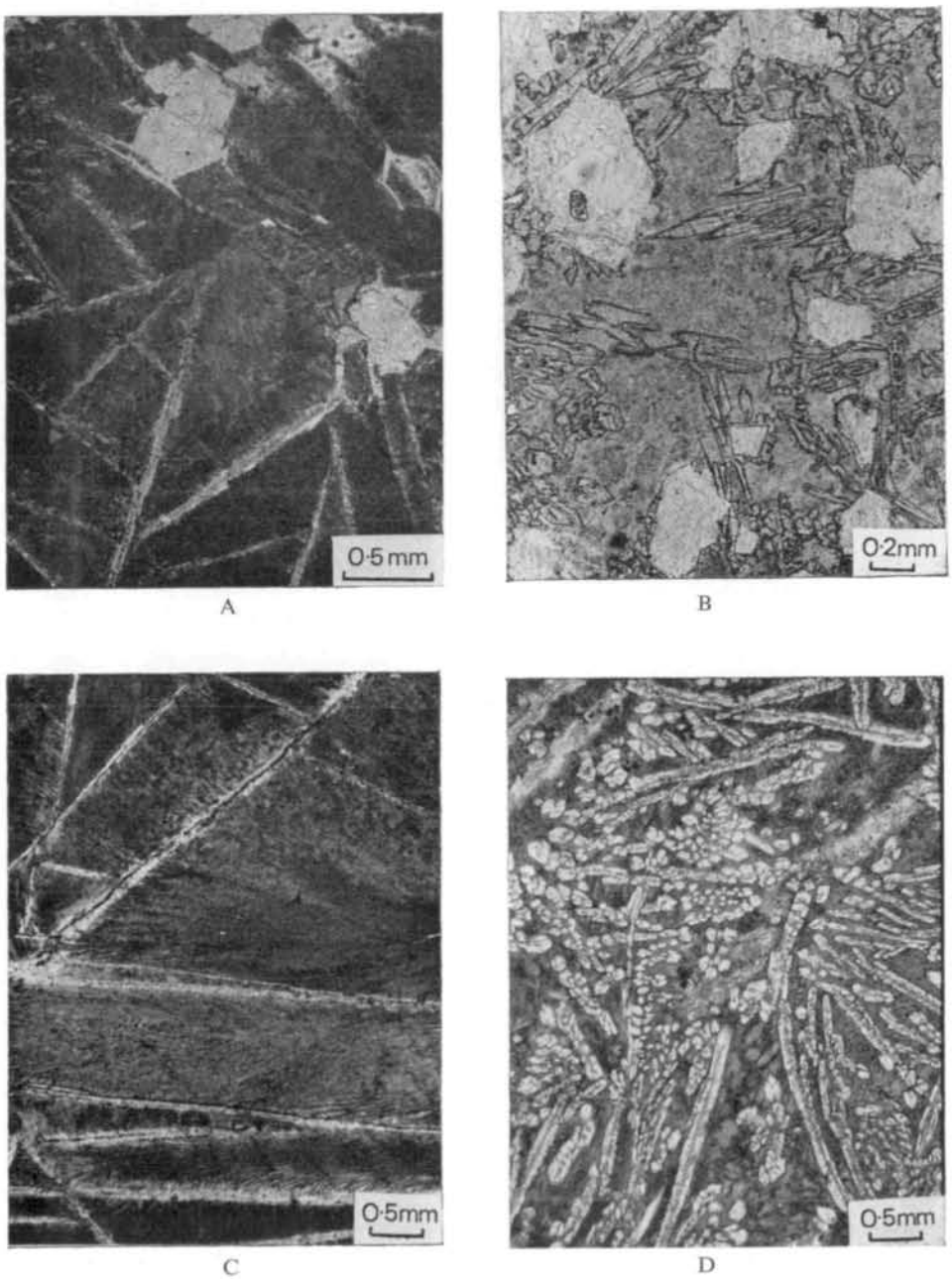

PLATE 3

PLATE 3A. Rapidly cooled olivine-rich pyroxenitic komatiite (P9-171), description in text.
PLATE 3B. Slowly cooled olivine-rich pyroxenitic komatiite lava (P9-185), description in text.
PLATE 3C. Rapidly cooled olivine-poor pyroxenitic komatiite lava (P9-234), description in text.
PLATE 3D. Slowly cooled olivine-poor pyroxenitic komatiite lava (P9-235), description in text.

Downloaded from https://academic.oup.com/petrology/article-abstract/18/2/319/1565696 by University of California, San Diego Library user on 28 March 2019

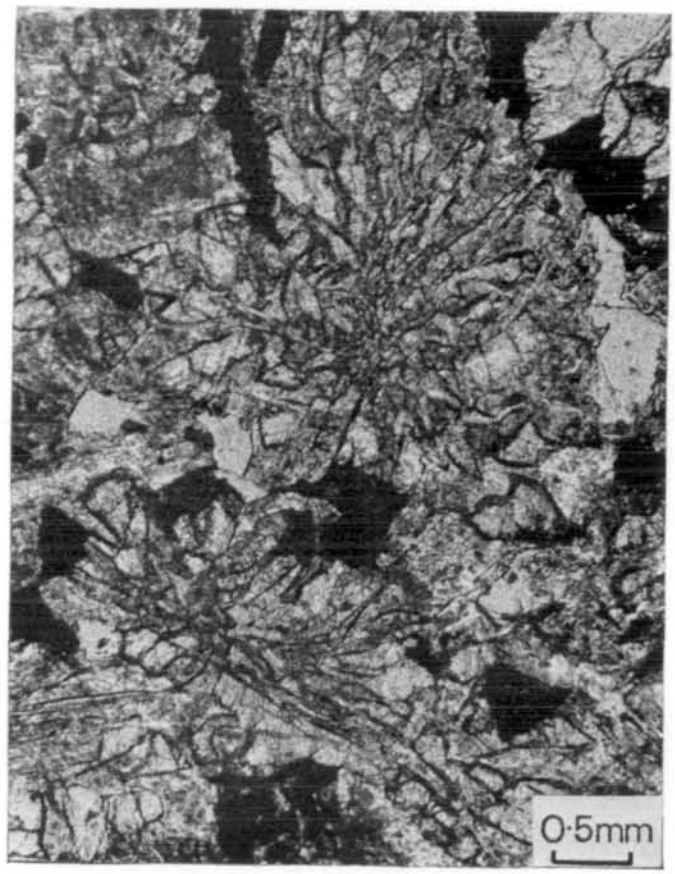

PLATE 4

PLATE 4. Clinopyroxene–plagioclase intergrowth in basaltic komatiite lava.

flow discussed (Fig. 7A) except that most of the spinifex texture is of the randomly oriented type rather than the sub-perpendicular type. The B_1 zone is missing, and equant crystals of presumed phenocryst olivine occur in amounts of 0 to 20 per cent in the lower part of the spinifex-textured zone. The proportion of equant olivine increases downward and where it exceeds 30–40 per cent, the rock appears massive in hand specimen, and skeletal or platy olivine is restricted to overgrowths on the equant grains. Small schlieren with fine-grained spinifex texture characteristically occur in a zone 1–2 m thick immediately below the spinifex zone. These schleiren commonly are subparallel to the plane of the flow and have a crescent shape, concave upward. They are 2–10 cm thick and 50 cm to several meters long. Some appear to be discrete, isolated bodies; others connect with cross-cutting veins that can be traced into the overlying spinifex zone (Plate 2B).

The proportion of equant olivine increases downward to a maximum of 60–70 modal per cent, three quarters of the way through the flow, before de-

Downloaded from https://academic.oup.com/petrology/article-abstract/18/2/319/1565696 by University of California, San Diego Library user on 28 March 2019

creasing towards the bottom. The lowermost few centimeters consist of a rock with less than 50 per cent olivine phenocrysts and a matrix of acicular, non-skeletal pyroxene grains, some of which are fractured or bent, some skeletal pyroxene and chlorite after glass.

Flows with limited or no spinifex texture commonly are made up of lava toes or lava lobes. Examples at Pyke Hill of lava toes in flows devoid of spinifex texture are described by Pyke *et al.* (1973). To the east of the Hedman Mine

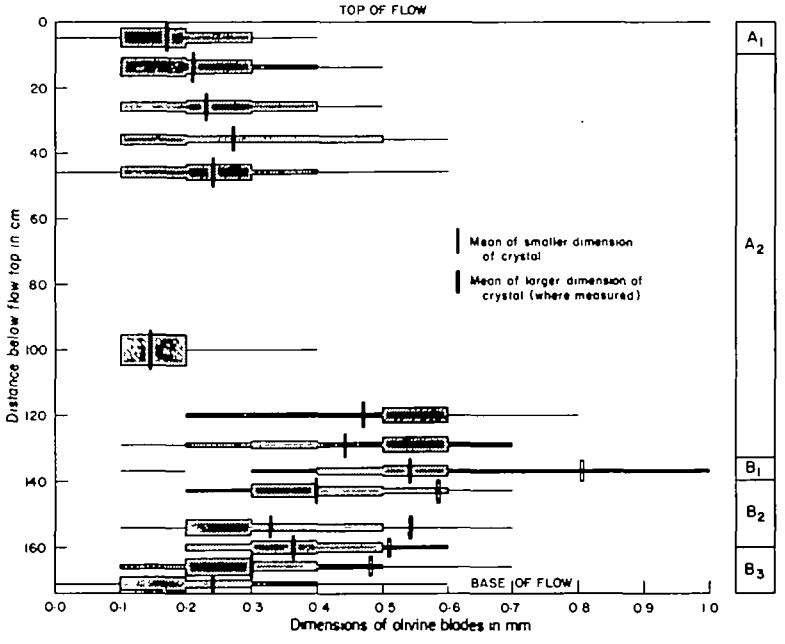

FIG. 8. Size variation of olivine grains in a spinifex-textured periodotitic komatiite flow. Histograms represent measurements in thin sections of the smaller dimension of the olivine grains. In the cumulus (B) zone the means of both the large and small dimensions are shown; in the spinifex zone the large dimension usually was greater than the size of the thin section and could not be measured.

road (Figs. 2 and 3) lava lobes with spinifex texture have been mapped. These lobes are large (2–6 m across) and crudely cylindrical, with convex upper surfaces and roughly concave or cusp-shaped lower surfaces that are moulded to conform to the shape of underlying lobes. Each lobe has a basal concentration of equant olivine grains, overlain, and to some extent concentrically surrounded, by a zone of spinifex texture and a curved, chilled, polyhedrally-jointed upper crust.

At Pyke Hill, sequences of spinifex-textured flows alternate with sequences of flows devoid of spinifex texture (Fig. 6). Individual flows are mainly of one type or the other, but in some, spinifex-textured upper zones become thicker and thinner in an irregular manner, or disappear entirely along strike. A more systematic variation occurs in a flow in the north of the Township (Fig. 3). This

Downloaded from https://academic.oup.com/petrology/article-abstract/18/2/319/1565696 by University of California, San Diego Library user on 28 March 2019

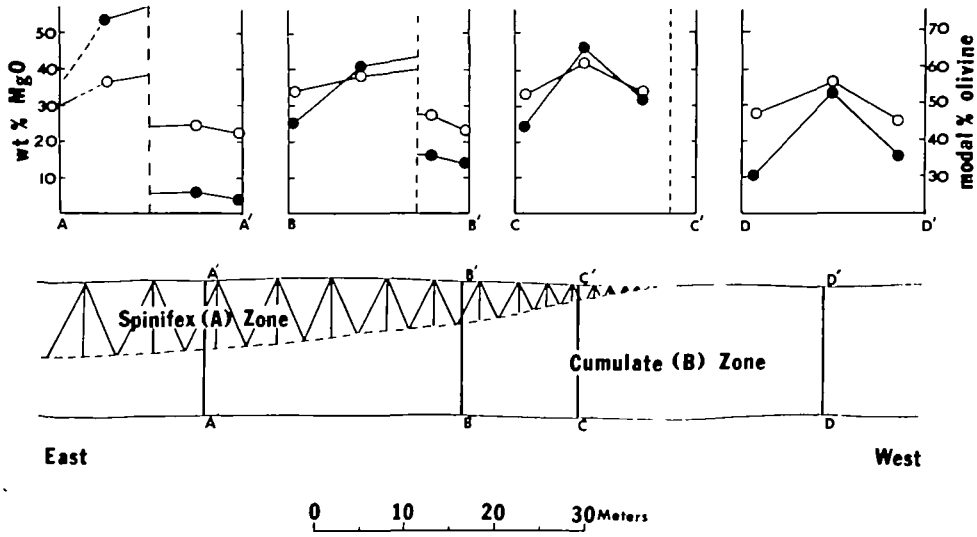

FIG. 9. Variation in MgO (*open circles*) and modal olivine (*closed circles*) in a peridotitic komatiite flow that grades from spinifex-textured in the east to spinifex-free in the west. The scale represents horizontal distance; flow is about 2 m thick.

flow is the lowermost of the second cycle (Fig. 5) and is relatively thin and spinifex-textured at its eastern end (Fig. 9). To the west the spinifex zone becomes thinner, then disappears entirely. Olivine distribution in the spinifex-textured eastern portion is as described above, whereas in the spinifex-free portion there is a central concentration of olivine that may reflect 'flowage differentiation' (Bhattacharji, 1967). Overlying spinifex-free flows show little variation in olivine content from top to bottom.

Mineral compositions

Analyses of minerals in samples SA 1157 to SA 2060, P9–103 to P9–239 and Min 12 were performed on an Applied Research Laboratories E.M.X. electron microprobe at the University of Toronto, using standard wavelength dispersion techniques. All elements were determined using a 15 kV accelerating voltage, a beam current of 0·3 to 0·5 mA, a beam size of 10–15 μm, and 10 second counting time. Data were processed with the EMPADR program (Rucklidge & Gasparrini, 1969). Samples SA 3054 to 3080 were analysed at the Geological Survey of Canada using an energy dispersive system.

Olivine

Nine representative analyses of olivine are given in Table 2. Forsterite content ranges from 85 to 94 mole per cent. The NiO content is high, ranging from 0·32 to 0·55 per cent and shows a rough positive correlation with forsterite content. Cr_2O_3 is unusually high, ranging from 0·14 to 0·33 weight per cent, and resembles that of lunar rather than terrestrial olivine (Meyer, 1975; Green *et al.*, 1975).

Downloaded from https://academic.oup.com/petrology/article-abstract/18/2/319/1565696 by University of California, San Diego Library user on 28 March 2019

TABLE 2

Average electron microprobe analyses of olivine (weight per cent)

A	*SA 1157*	*SA 2041*	*SA 1158*	*SA 2048*	*SA 3056*	*SA 2039*	*SA 2047*	*SA 2059*	*SA 3062*
B	A_1	A_1	A_2	A_2	A_2	B_1	B_2	B_2	B_4
SiO_2	41·1	39·4	41·8	40·5	41·2	39·2	40·8	40·8	40·8
FeO^t	8·2	8·8	9·8	11·4	13·8	11·3	6·6	8·1	6·1
MgO	50·2	51·0	48·2	48·1	44·1	48·8	52·6	51·0	51·5
CaO	0·25	0·20	0·27	0·27	n.d.	0·30	n.d.	0·26	n.d.
Cr_2O_3	0·23	0·19	0·21	0·33	0·27	0·27	0·14	0·29	0·22
NiO	n.d.	0·46	n.d.	0·40	n.d.	0·38	0·55	0·39	n.d.
TOTAL	100·00	100·1	100·3	101·0	99·37	100·3	100·7	100·8	98·60
Fo	0·916	0·912	0·897	0·883	0·851	0·885	0·934	0·918	0·938
N	3	15	2	11	4	15	16	10	3

Notes A—Sample number.
B—Section of flow sampled (see Fig. 7).
N—number of analyses in average.
n.d.—not determined.

TABLE 3

Microprobe analyses of pyroxene in komatiitic lavas

	1 *SA 1162*	*2* *SA 2041*	*3* *SA 2044*	*4* *SA 2051*	*5* *SA 2053*	*6* *SA 2056*	*7* *SA 2057*	*8* *P9 118*	*9* *P9 139*	*10* *P9 1336*	*11* *P9 235*	*12* *Mun 12*
SiO_2	48·8	47·7	47·1	47·9	48·5	49·00	50·0	49 5	51·8	47·5	49·1	51·6
Al_2O_3	8·5	8·2	8 6	7·8	7·5	7·3	7·0	5·7	4·4	8·6	8·8	3·10
TiO_2	n.d.	0·95	0·86	0·96	0·51	0·68	0·63	0 44	0·62	0·50	1·17	·0·35
FeO*	7·1	8·4	8 6	8 3	10·4	7·2	6·5	8·5	9·9	11·4	7·43	9·48
MnO	n.d.	0 04	0·07	0 07	0·29	0·0	0 01	n.d.	n.d.	0 25	n.d.	0·21
MgO	14·3	13 2	13 1	12·4	15·1	14·7	16 5	17 0	14·6	15·6	12·9	17·7
Cr_2O_3	0·47	0·39	0·35	0·38	n.d.	0·46	0·28	n.d.	n.d.	n.d.	n.d.	n.d.
CaO	21·1	20·2	20·3	21·6	18·0	20·4	20·1	18 6	20·1	16·3	20·3	·17·2
Na_2O	n.d.	0·20	0·19	0·17	0·20	0·17	0 17	n.d.	n.d.	n.d.	n.d.	0·13
TOTAL	100·27	99 28	99·17	99·58	100·50	99·91	101·4	99·8	101·6	100·2	99·7	99·9
N	2	7	8	8	7	8	8	2	8	9	3	5
	Recalculated on Basis of 24 Oxygen Atoms											
Si	7·18	7·14	7 07	7 17	7·19	7·24	7·26	7·33	7·58	7·06	7·23	7·63
Al	0·82	0 86	0·93	0·83	0·81	0·76	0·74	0·67	0·42	0·94	0·76	0·34
Al	0·66	0·59	0·59	0·55	0·50	0·51	0·46	0·32	0·34	0·56	0·76	0·17
Ti	n.d.	0·11	0·10	0·11	0·06	0·08	0·07	0·05	0·07	0·06	0·13	0·04
Fe	0·87	1·05	1·08	1·04	1 29	0 89	0·79	1·06	1·22	1·43	0·93	1·17
Mn	n.d.	0·00	0·01	0·01	0 00	0·00	0·00	n.d.	n.d.	0·03	n.d.	0 03
Mg	3·14	2·94	2·93	2·77	3·34	3·24	3·57	3·75	3·18	3·45	2·83	3·90
CO	0·06	0 04	0·04	0·04	n.d.	0·05	0·03	n.d.	n.d.	n.d.	n.d.	n.d.
Ca	3·33	3·27	3 27	3·46	2·86	3·23	3·12	2·95	3·15	2·60	3 21	2·72
Na	n.d.	0·06	0·06	0·05	0·06	0·05	0·05	n.d.	n.d.	n.d.	n.d.	0·04
TOTAL	16·06	16 06	16·08	16·03	16·11	16·05	16·09	16·13	15·96	16·13	15·85	16·04
Wo	45·3	44·8	44·9	47·6	38·2	43·9	41·8	38·0	41·7	34·7	46·1	34 9
En	42·8	40·7	30·3	38·1	44·6	44 0	42·7	48 3	42·1	46·2	40·5	50·0
Fs	11·9	14·5	14·8	14·3	17·2	12·1	10·5	13·7	16·2	19·1	13·3	15·0

1 to 10 Skeletal clinopyroxene needles from spinifex-textured peridotitic komatiite lava.
11 Skeletal clinopyroxene grains from groundmass of pyroxenitic komatiite lava.
12 Subhedral prismatic clinopyroxene from sub-ophitic basaltic komatiite lava.

Downloaded from https://academic.oup.com/petrology/article-abstract/18/2/319/1565696 by University of California, San Diego Library user on 28 March 2019

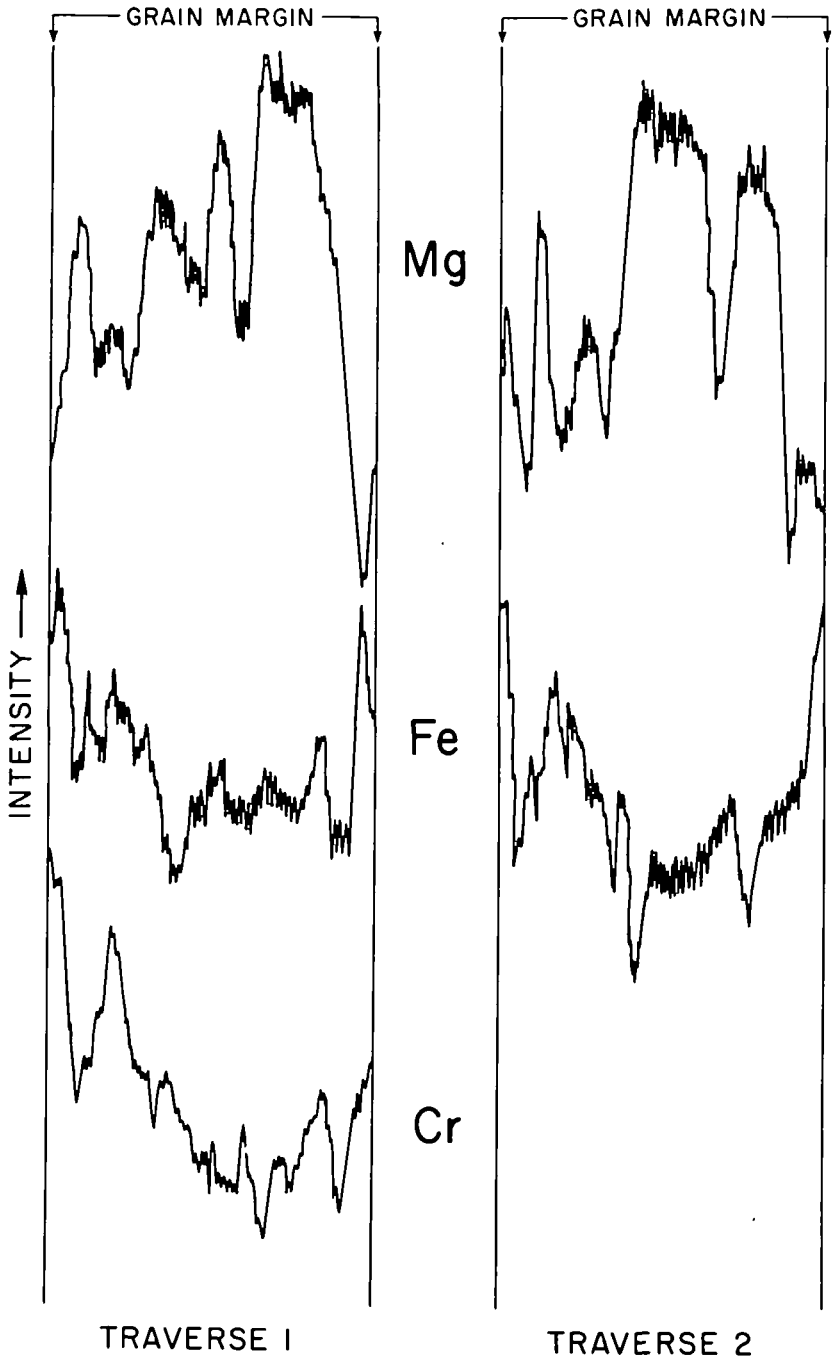

FIG. 10. Two electron microprobe traverses across an olivine grain illustrating variations in composition.

Downloaded from https://academic.oup.com/petrology/article-abstract/18/2/319/1565696 by University of California, San Diego Library user on 28 March 2019

The CaO content of the 8 samples for which this was determined ranges from 0·2 to 0·3 weight per cent.

Qualitative microprobe profiles of Fe, Mg, and Cr across a bladed olivine from spinifex texture (Fig. 10) demonstrate the zoned nature of the grain. A series of spot analyses across the blade, but not on the traverse shown in the figure, revealed an increase in forsterite from 89·5 to 91·1 mole per cent, and a decrease in Cr_2O_3 from 0·32 to 0·23, from edge to center of the grain.

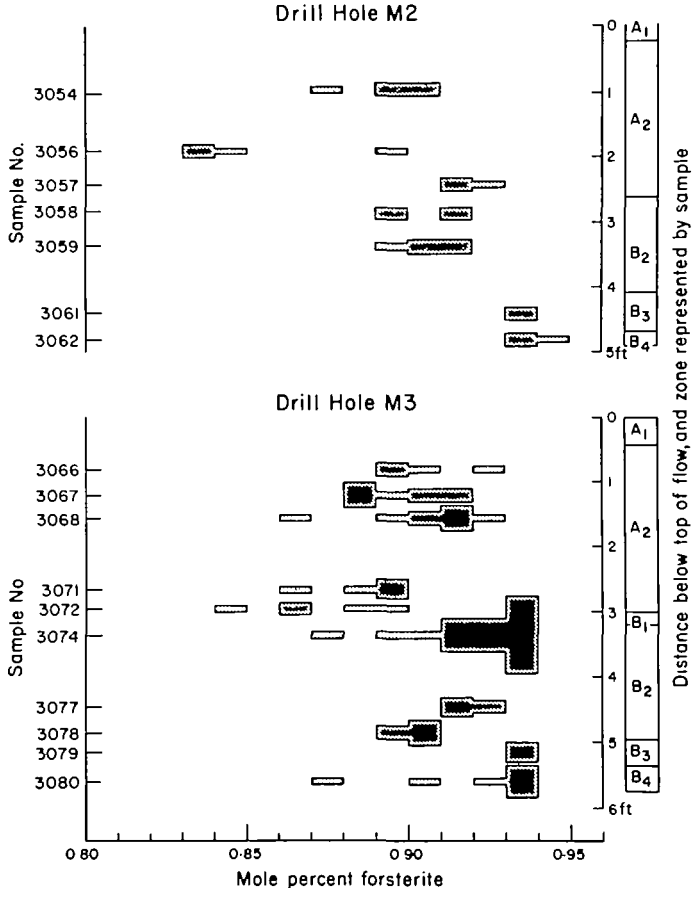

FIG. 11. Variation in the olivine composition in two drill holes through a spinifex-textured peridotiti komatiite flow.

Variation in forsterite content along two drill holes through a single spinifex-textured flow is illustrated in Fig. 11. The zoning within many samples reduces the confidence with which one can generalize about compositional variation across the flow itself, but the data do suggest that the average composition of olivine in the B zone is similar to that of olivine in the upper part of the A_2 zone, and that olivine in the lower part of the A_2 zone is slightly less forsteritic. From Fig. 12 it can be seen that no systematic relationship exists between the forster-

Downloaded from https://academic.oup.com/petrology/article-abstract/18/2/319/1565696 by University of California, San Diego Library user on 28 March 2019

ite content of olivine and the stratigraphic height in the entire sequence exposed at Pyke Hill. The cumulus olivine in the thick (18 m) basal flow of the sequence (analysis SA 2039) is distinctly less forsteritic than phenocryst olivine trapped in the upper chill zone. This anomaly corresponds with anomalies in the bulk compositions of zones in this flow and will be discussed later.

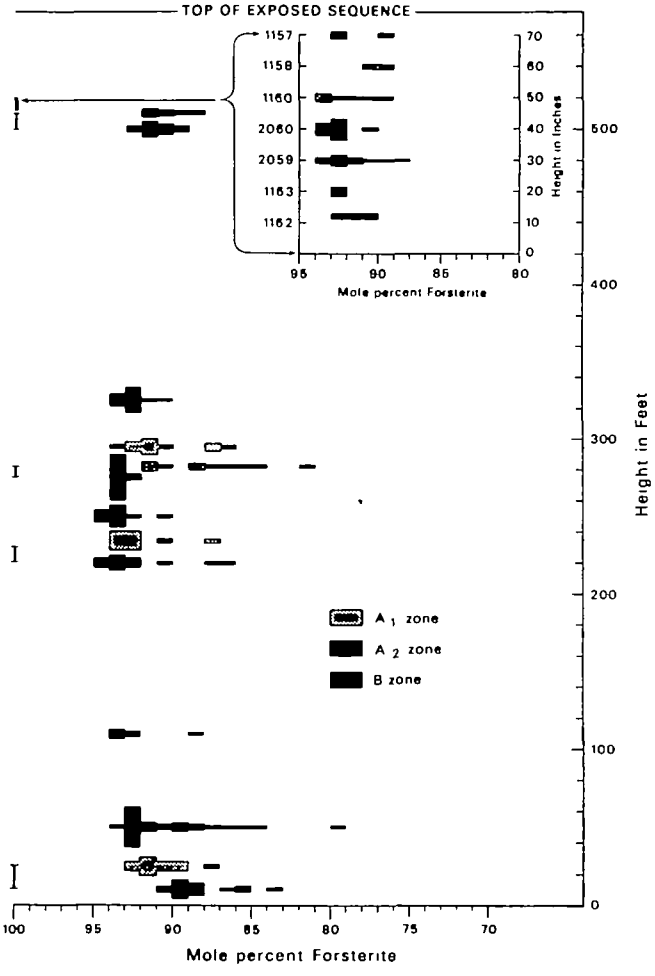

FIG. 12. Olivine composition variation in peridotitic komatiite flows of Pyke Hill. The thickness of the bars is proportional to the number of analyses, and the brackets to the left signify two or more samples from different zones of the same flow.

Pyroxene

Pyroxenes interstitial to olivine grains have sub-calcic augite compositions (Table 3). They are highly aluminous with substantial Al^{3+} in tetrahedral coordination. Strong zoning in all grains results in considerable variation in CaO, FeO, and MgO contents. The grains are skeletal or highly acicular and are

Downloaded from https://academic.oup.com/petrology/article-abstract/18/2/319/1565696 by University of California, San Diego Library user on 28 March 2019

thought to represent disequilibrium crystallization from supercooled liquid or glass. Hence, some chemical variation may be due to variation to differences in the degree of supercooling and the stage at which pyroxene grew.

Chromite

Chromites of spinifex and cumulus zones have MgO contents between 3·8 and 14·3 weight per cent, and Cr_2O_3 contents between 39·5 and 56·2 weight per cent (Table 4). Most analyses are of equant grains because of the difficulty

TABLE 4

Microprobe analyses of chromite

	SA 1162	*SA 1163*	*SA 2040*	*SA 2041*	*SA 2044*	*SA 2053*	*SA 2054*	*SA 336a*	*SA 336b*
MgO	11·7	14·3	4·20	13·5	11·8	12·9	3·76	12·3	13·4
FeO*	16·7	12·5	27·9	13·4	16·5	14·6	28·3	14·9	13·8
MnO	0·30	0·24	0·52	0·32	0·47	0·42	0·96	0·52	n.d.
Fe_2O_3*	3·92	3·28	7·03	5·26	7·92	7·92	14·0	7·70	9·01
Al_2O_3	15·0	14·0	13·9	12·8	14·4	14·0	13·8	14·6	13·9
Cr_2O_3	53·0	56·2	46·8	54·9	50·3	50·9	39·5	48·9	49·4
TiO_2	0·31	0·26	0·45	0·34	0·35	0·37	0·69	0·39	0·41
TOTAL	100·9	100·7	100·8	100·5	101·7	101·1	101·0	99·3	99·9

n.d.—not determined.

* Iron was analysed as FeO and proportioned between Fe^{2+} and Fe^{3+} on the assumption of a stoichiometric formula for the spinel, and assuming TiO_2 substitutes as in ulvospinel.

SA 1162 Equant euhedral grain, cumulate zone, peridotitic komatiite lava.
SA 1163 „ „ „ „ „ „ „
SA 2040 „ „ „ spinifex zone, „ „ „
SA 2041 „ „ „ flow top, „ „ „
SA 2044 „ „ „ „ „ „ „
SA 2053 „ „ „ spinifex zone, „ „ „
SA 2054 „ „ „ cumulate zone, „ „ „
P9-336a Skeletal grain, spinifex zone, „ „ „
P9-336b Equant euhedral grain „ „ „ „ „

of analysing the fine skeletal grains. Despite their euhedral form, the observations (1) that chromite is observed enclosed in phenocryst olivine and (2) that the highest Cr contents are in rocks containing intermediate (18–25 per cent) MgO concentrations lead to the conclusion that chromite did not crystallize at an early stage, probably not starting until after much olivine had crystallized. Consequently, the chromite may have crystallized out of equilibrium with its host magma.

Matrix

The compositions of the devitrified and chloritized glass that forms the matrix in spinifex-textured and massive lavas (Table 5) range from that of a peridotitic komatiite (SA 2054; 24 per cent MgO) to an extremely MgO-poor

Downloaded from https://academic.oup.com/petrology/article-abstract/18/2/319/1565696 by University of California, San Diego Library user on 28 March 2019

basaltic komatiite composition (P9-236; 3·3 per cent MgO). The variation in matrix compositions may in part be a result of migration of elements during devitrification, or may reflect inhomogeneities induced within the residual liquid during disequilibrium crystallization of olivine and pyroxene.

TABLE 5

Defocussed-beam microprobe analyses of interstitial devitrified glass

	1	*2*	*3*	*4*	*5*	*6*	*7*	*8*	*9*	*10*
SiO_2	48·0	41·9	40·5	43·3	43·4	42·6	46·2	43·1	44·9	49·6
Al_2O_3	14·5	13·1	10·1	11·6	12·8	11·7	10·7	17·3	10·3	12·2
TiO_2	0·47	0·50	0·52	0·63	0·66	0·63	n.d.	0·62	n.d.	0·54
FeO*	10·9	10·2	8·5	10·7	14·5	12·2	12·6	7·4	12·4	9·0
MnO	0·36	0·27	0·23	0·24	0·41	0·43	0·30	0·25	0·28	n.d.
MgO	3·29	18·7	24·0	16·8	10·8	11·9	12·4	14·9	15·3	17·9
CaO	14·0	4·9	7·7	12·8	10·2	13·5	13·1	7·1	11·9	2·19
Na_2O	n.d.	1·24	0·71	1·32	2·01	1·87	2·10	2·89	1·53	n.d.
K_2O	n.d.	0·55	0·62	0·22	0·06	0·06	0·12	0·25	0·12	n.d.
TOTAL	91·5	91·4	92·9	97·6	94·8	94·9	97·5	93·8	96·7	91·4
N	6	3	4	5	4	5	4	5	4	2

* FeO—total iron as FeO.
n.d.—not determined.
N—number of analyses.
P9-236 spinifex-textured peridotitic komatiite lava.
P9-115 center, spinifex-free peridotitic komatiite lava.
SA 2054 cumulate zone spinifex-bearing peridotitic komatiite lava.
SA 2059 ,, ,, ,, ,, ,, ,, ,,
SA 2050 flowtop ,, ,, ,, ,, ,, ,,
SA 2060 cumulate zone ,, ,, ,, ,, ,,
SA 1158 ,, ,, ,, ,, ,, ,, ,,
SA 2056 ,, ,, ,, ,, ,, ,, ,,
SA 1157 ,, ,, ,, ,, ,, ,, ,,
P9-235 center, massive pyroxenitic komatiite flow.

Chemical variation within individual flows

Figure 13 shows the variation in Al_2O_3, CaO, and MgO along two holes drilled 7 m apart in a flow with well-developed spinifex texture. In both profiles there is (a) a slight decrease in MgO and an increase in CaO and Al_2O_3 across the A_1 and A_2 zones, (b) an abrupt increase in MgO and decrease in CaO and Al_2O_3 at the contact between the A_2 zone and the underlying B zone, and (c) a progressive decrease in MgO and increase in CaO and Al_2O_3 across the lower half of the B zone. The B_3 zone has distinctly less MgO than the B_2 zone. In Table 6 compositions of the A_1, A_2, B_2, B_3, and B_4 zones (averages in the case of A_2 and B_2) are compared. Relatively little difference exists between them, and, in particular, the A_2 zone has essentially the same composition in each.

Figure 13 also shows variation of the same elements along a hole drilled through a flow showing only limited spinifex texture development. This profile differs from the others in the progressive increase in MgO and progressive

Downloaded from https://academic.oup.com/petrology/article-abstract/18/2/319/1565896 by University of California, San Diego Library user on 28 March 2019

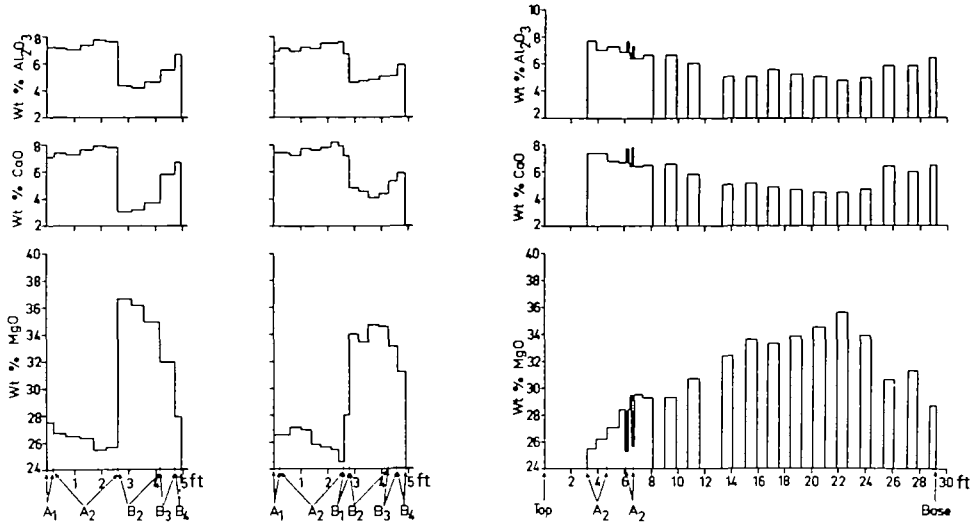

FIG. 13. MgO, CaO, and Al_2O_3 variations in (a) two flows with well-developed spinifex zones (*left*) (b) a flow with poorly developed spinifex zone (*right*).

decrease in CaO and Al_2O_3 to about three-quarters of the way through the flow, followed by a reversal in the trend over the lowermost 2 meters. Two small schlieren with spinifex texture that were intersected just below the base of the main spinifex zone are very similar in composition to the main spinifex zone. The chemical variations in all profiles correspond closely to the distribution of olivine observed in the field and in thin section.

Figure 9 illustrates variation in MgO content in the flow that changes from spinifex-textured to massive. Profiles in the spinifex-textured portions correspond to those of the drill sections. In the massive, spinifex-free section MgO is concentrated towards the center of the flow paralleling the olivine distribution. Total MgO and olivine content decreases slightly from east to west.

TABLE 6

Comparison of two drill sections 7 m apart through a single peridotitic komatiite flow

Zone	Hole No.	No. of Anal.	SiO_2	Al_2O_3	FeO*	MgO	CaO	Na_2O	K_2O	TiO_2	MnO	Cr_2O_3	NiO
A_1	M_2	1	46·0	7·21	10·4	27 5	7·08	0·42	0 13	0·27	0·19	0·39	0·05
	M_3	1	45 4	6·93	11·3	26 5	7·36	0·37	0·15	0·27	0·21	0 23	0·05
A_4(Av)	M_2	5	45·9	7·32	11·1	26·1	7 59	0·70	0·10	0·31	0 21	0·28	0·05
	M_3	7	45·7	7·28	11·3	26·0	7·69	0·69	0 09	0·29	0·20	0·20	0·07
B_2(Av)	M_2	3	44·8	4·34	10·1	35·9	3·33	0·13	0·01	0·12	0·15	0·20	0·05
	M_3	4	45·0	4·82	9·87	34 2	4·46	0·12	0·04	0·15	0·19	0·17	0·17
B_3	M_2	1	45·1	5·47	10·4	31·9	5·83	0·29	0·07	0·19	0·18	0·20	0·05
	M_3	1	44 6	5·06	9·76	33·1	5·29	0·29	0·04	0·17	0·18	0·19	0·16
B_4	M_2	1	46 0	6·71	10·8	27·9	6·73	0·26	0·11	0 28	0·19	0·21	0·05
	M_3	1	45·5	5·91	10·7	31·2	5 92	0·40	0·08	0·21	0·19	0·16	0·16

Downloaded from https://academic.oup.com/petrology/article-abstract/18/2/319/1565696 by University of California, San Diego Library user on 28 March 2019

Discussion of formation and crystallization of flows

The flows in Munro Township, in common with all Archean ultramafic flows known to the authors, occur within a sequence of pillowed basalts and cherty sediments indicative of extrusion under water. The contrast in habit between the equant and spinifex olivine indicates that the two have crystallized under different conditions, probably related to the difference in cooling rate, the presence or absence of nucleii, and hence the degree of supersaturation of the magma (Lofgren, 1974; Donaldson, 1974; Walker *et al.* 1976). The skeletal and bladed crystals are thought to be produced by rapid cooling of lava devoid of phenocrysts, and their exact form is probably related to the cooling rate itself. The equant olivine crystals are thought to have formed under conditions of somewhat slower cooling in which original phenocrysts were available to act as nucleii.

Considering first the flows with well-developed spinifex texture, the polyhedrally-jointed cap-rock is interpreted as a chill zone that formed immediately on extrusion. Once horizontal flow replaced the near-vertical flow up the feeder conduit, olivine phenocrysts suspended in the lava settled rapidly to form the cumulus B zone, leaving a zone of lava devoid of phenocrysts between the cap-rock and the top of the cumulus zone. The downwards decrease in grainsize in the cumulus zone (Fig. 8) is explained if one assumes that the phenocrysts were growing rapidly at this time. Those at the base of the zone accumulated first and would have had less time to grow than those at the top of the zone.

The combination of rapid cooling from the top downwards, and the absence of suitable nucleii for crystallization except at the top, resulted in supersaturation of the lava, and consequently olivine blades crystallized rapidly downward from overlying nucleii, giving rise to the spinifex texture. Although spinifex texture in normal flows probably grows at a stage when movement of the flow has largely ceased, the presence in some lava lobes of this texture concentrically distributed around a core of cumulate olivine suggests that growth also may occur while the lava is still moving.

An assumption in this interpretation is that spinifex-textured rock represents the composition of the liquid portion of a given lava. The slight but consistent decrease in MgO (1 to 2 per cent), and the increase in CaO (0·5 to 0·7 per cent) and Al_2O_3 (0·5 to 0·6 per cent) downwards across the A_2 zone in the drill hole (Fig. 13), as well as the suggestion of a parallel decrease in the forsterite content of olivine (Fig. 11), indicate that limited crystal–liquid fractionation probably occurred during crystallization of the spinifex zone, with MgO becoming enriched in the upper, earlier crystallization portion of the A_2 zone. In thin flows such as the one intersected by the drill holes, this fractionation is slight and a single sample probably gives a close approximation to the liquid portion of the flow. However, the average of a series of samples across the whole zone is regarded as being more representative than a single sample. The very similar

Downloaded from https://academic.oup.com/petrology/article-abstract/18/2/319/1565696 by University of California, San Diego Library user on 28 March 2019

average composition obtained for the A_2 zone from each of the two holes lends support to this view. Although the cap-rock provides a composition of the lava, it does not represent a liquid composition because it contains olivine phenocrysts.

Green *et al.* (1975) argued on the basis of experimental results and on the absence of vesicles in komatiitic lavas that peridotitic komatiite lavas are dry. If such is the case, a liquid with the composition of the A_2 zone would erupt at 1450 to 1500 °C (Shima & Naldrett, 1975; Arndt, 1976*a*) and would have a viscosity of about 10 poises (from the data of Bottinga & Weill, 1972). Assuming a density difference of 0·4 between crystals and liquid, an olivine grain 0·5 mm in diameter would settle at a terminal velocity of 40 cm per hour. The same grain in a dry basaltic liquid at 1200 °C would have a terminal velocity of only 0·04 cm per hour. The sharp separation between spinifex and cumulate zones in many peridotitic komatiite flows is explained in this way.

The gradual decrease in olivine over the basal meter of the flows is attributed to two factors: 'flowage differentiation' (Bhattacharji, 1967), which keeps phenocrysts concentrated at the center of the flow; and chilling at its base, which raises the viscosity and reduces the rate of settling within this zone once flow has ceased.

The differences between the flow types illustrated in Fig. 7 are believed to result from different degrees to which gravitational settling has separated olivine phenocrysts from liquid lava. Spinifex texture only develops in liquids essentially devoid of phenocrysts. Thus, the type of flow with a thick spinifex-textured zone is the result of complete separation; the intermediate flow type is a result of solidification of the lava before complete separation; and the spinifex-free flow type is a result of solidification with little or no gravity settling. The disappearance of spinifex texture in the flow shown in Fig. 9 is interpreted as follows: volcanic structural criteria such as the direction of thinning of flows, and the orientation of lava lobes indicate that in the north of the Township, flowage direction was from west to east. Close to the conduit olivine phenocrysts could settle in hot, fluid lava, and spinifex texture could form, but as the lava flowed eastward it cooled, its viscosity increased, and the settling of olivine grains first was inhibited, then prevented.

PYROXENITIC KOMATIITES

Included in this category are lavas with a wide range of textures, mineralogy, and chemical composition. Some flows are rich in equant phenocrysts or fine, acicular, skeletal grains of olivine, and others are composed mainly of pyroxene. Textures range from porphyritic, to spinifex, to cumulus and are related both to the composition and the cooling history of the lava.

Pyroxenite komatiites will be described with reference to Table 1, which gives a definition of the rock type and a brief account of the main features, and Fig. 14, which shows diagrammatic sections of two flows and sketches of typical tex-

Downloaded from https://academic.oup.com/petrology/article-abstract/18/2/319/1565696 by University of California, San Diego Library user on 28 March 2019

tures. Flows of this type tend to be thicker than their peridotitic counterparts, ranging from 5 to 15 m thick, and they generally can be traced hundreds of meters in areas of good outcrop.

Olivine-rich varieties (Fig. 14*a*) usually are massive and relatively featureless, although lava toes occur, flowtops may be brecciated or spinifex-textured, and the entire flow may be polyhedrally jointed. Near the flowtop, olivine occurs as equant phenocrysts with skeletal overgrowths, as discrete, prismatic grains, and as very thin, randomly-oriented wafers, which are set in a matrix of acicular, dendritic or plumose clinopyroxene, sparse minute euhedral grains of chromite, and devitrified glass. Plate 3A is a photomicrograph of this type of lava.

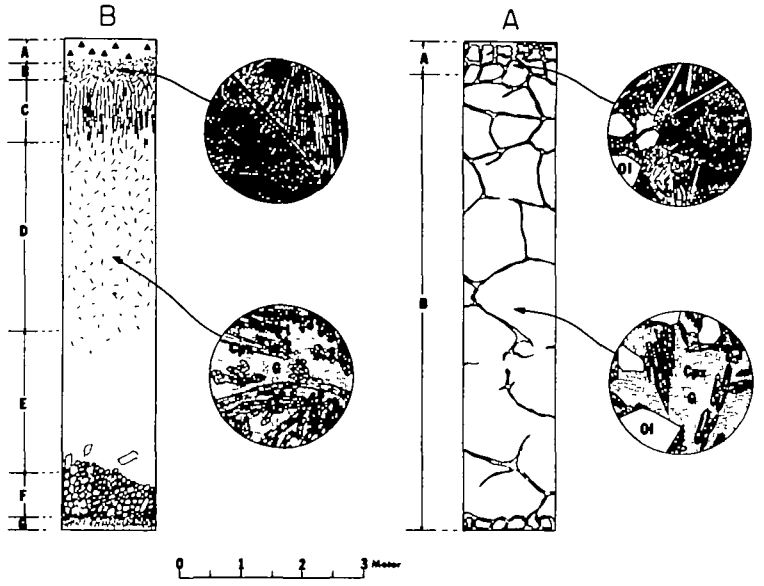

FIG. 14. Diagrammatic sections through two pyroxenitic komatiite flows and sketches of portions of thin sections. Flow B contains the following units: (A) flowtop breccia, (B) random olivine-bearing spinifex texture, (C) parallel clinopyroxene spinifex texture, (D) random microclinopyroxene spinifex texture, (E) medium-grained equigranular rock, (F) clinopyroxene±orthopyroxene±olivine cumulate, (G) basal clinopyroxene spinifex texture. Flow A contains an (A) upper chilled and polyhedrally jointed flow top, and (B) a major zone of more slowly cooled lava. Ol—olivine; cpx—clinopyroxene; G—devitrified glass.

The centers of olivine-rich flows contain only solid, equant olivine grains; elongate, skeletal, and wafer-shaped grains are missing. Clinopyroxene grains are coarser than those in the flowtop and form discrete, skeletal rods and prisms with the unusual habits illustrated in Fig. 14 and Plate 3B. Representative analyses of clinopyroxene and devitrified glass in pyroxenitic komatiites are listed in Tables 3 and 5. Olivine invariably is serpentinized and could not be analysed.

The contrast in grainsize and texture between flowtop and flow center is ascribed to differences in cooling rate. The large, equant, solid olivine grains in both zones are phenocrysts that formed under conditions of relatively slow cool-

Downloaded from https://academic.oup.com/petrology/article-abstract/18/2/319/1565696 by University of California, San Diego Library user on 28 March 2019

ing and were transported into place. Grains of olivine and clinopyroxene that grew in place in the flowtop are small and have plumose or dendritic habits characteristic of rapid cooling rates, whereas grains that grew at the centers of flows are coarser, less skeletal, and are acicular or prismatic. The variation in habit is consistent with the results of experimental studies by Lofgren *et al.* (1974), Donaldson (1974) and Walker *et al.* (1976) that relate crystal habit to cooling rate.

Flows rich in pyroxene and poor in, or devoid of, olivine exhibit a wide range of volcanic structures and textures such as are illustrated in the composite flow, Fig. 14b. Not all the features shown are present in every flow, and many are much simpler. Flowtops often contain very thin ($<100\mu$), randomly-oriented wafers of olivine, which are set in a matrix of fine-grained clinopyroxene and devitrified glass, and impart a distinctive 'criss-cross' texture to the rock (Plate 3C). This texture gives way downwards to textures made up of large needles of pyroxene that are oriented parallel to one another and perpendicular to the flowtop immediately below the zone of 'criss-cross' texture, and are randomly oriented closer to the centers of flows (Plate 3D). The clinopyroxene needles, which may be as long as 3 mm, but only 0·05 mm wide, are strongly zoned with cores richer in Mg and Al and poorer in Ca than margins (Table 3). Central cores in many grains are composed of chlorite that probably is pseudomorphic after Ca-poor clinopyroxene or orthopyroxene (Arndt, 1975). The large clinopyroxene needles lie in a matrix composed of smaller, prismatic clinopyroxene grains and devitrified glass. These textures are regarded as spinifex textures, even though the dominant mineral is pyroxene, not olivine. In some flows olivine spinifex texture typical of that described by Nesbitt (1971) and Pyke *et al.* (1973) grades down into pyroxene spinifex; the gross characteristics such as the skeletal crystal form and parallel grouping of the dominant mineral grains are the same in both types, and the factors that result in the formation of the textures are likely to be the same.

A thin interval of flowtop breccia may overlie the spinifex-textured zones (Fig. 14b), and an interval of cumulate rock composed of subhedral clinopyroxene grains, with or without orthopyroxene and olivine, may form the base of the flow. Other features of some pyroxene-rich pyroxenitic komatiites are varioles in flowtop zones, and polyhedral jointing.

BASALTIC KOMATIITES

The field characteristics of basaltic komatiites are compared with those of more mafic komatiites in Table 1. Flowtops are brecciated and in rare cases spinifex-textured, and the underlying lava is massive and medium-grained even in relatively thin flows, or is pillowed and finer grained. Individual flows range in thickness from less than 2 m to more than 20 m, and in some areas can be traced for 2 km, often changing intermittently over this distance from massive

Downloaded from https://academic.oup.com/petrology/article-abstract/18/2/319/1565696 by University of California, San Diego Library user on 28 March 2019

to pillowed. Other flows terminate in short distances, suggesting that most flows have a tongue-like form and are much longer in one direction than the other.

Textures in the more mafic varieties (Mg > 10 per cent) are similar to those in olivine-poor pyroxenitic komatiites. Parallel clinopyroxene spinifex texture in flowtops grades downwards into microspinifex texture in which the clinopyroxene needles are randomly oriented. However, olivine only is present as rare, highly-skeletal, equant phenocrysts and never as bladed grains in the groundmass, the clinopyroxene needles are smaller than those in pyroxenitic komatiites (their average length is 0·5 to 1 mm) and the groundmass to the needles is entirely devitrified glass or an intergrowth of prismatic grains of clinopyroxene and plagioclase.

Basaltic komatiites with lower MgO contents have textures and modal compositions not unlike those of non-komatiitic basaltic rocks. These lavas are composed of prismatic, subhedral grains of clinopyroxene ($En_{50}Fs_{18}Wo_{34}$) and plagioclase, some amphibole, quartz, and iron oxides. Serpentine or chlorite replace rare solid or skeletal phenocrysts of olivine or orthopyroxene. A characteristic texture is a mutual intergrowth of clinopyroxene and plagioclase (Plate 4), which, when well developed, has an appearance similar to graphic intergrowths of quartz and albite in pegmatites or graphic granites. Some basaltic komatiites are porphyritic with phenocrysts of clinopyroxene or plagioclase set in fine-grained groundmass of the same minerals.

In Warden Township, underlying the main succession of komatiites, a number of komatiitic flows that are less mafic than normal basaltic komatiites are interlayered with tholeiitic basalts. These flows, which could be called andesitic komatiites inasmuch as they have SiO_2 greater than 54 per cent and high normative and modal plagioclase contents, are harder and paler than basaltic komatiites but share most of their characteristic features: *i.e.* they may be massive or pillowed, they may have flowtop breccias, and in rare cases they have zones of a spinifex texture rich in plagioclase.

THOLEIITIC LAVAS

In Munro Township and in the surrounding areas, tholeiitic volcanic rocks of basaltic to andesitic composition occur in successions 500 to 1500 m thick alternating with slightly thinner successions of komatiitic lavas. Although some komatiitic flows may be intercalated with tholeiites at the interfaces between successions, each succession generally is made up of lavas of only one of the two series.

Most tholeiitic basalt flows are less than 10 m thick, although some in central Warden Township are over 100 m thick. They may be pillowed, or massive with brecciated flowtops, or entirely fragmental. Brecciation in some flows is a result of mechanical shattering during flowage; in others, differential contraction of glass to produce hyaloclastite appears to have been more important.

Downloaded from https://academic.oup.com/petrology/article-abstract/18/2/319/1565696 by University of California, San Diego Library user on 28 March 2019

Basaltic lavas are fine-grained and equigranular, or contain phenocrysts of clinopyroxene, or more rarely of plagioclase. Olivine is not present. Dominant minerals are subhedral, prismatic or stubby grains of clinopyroxene, ragged laths of altered plagioclase, and fine-grained iron oxide. Small anhedral grains of quartz, chlorite in anhedral patches, and amphiboles are present in smaller amounts. Samples from the margins of flows or pillows usually are made up of a fine-grained intergrowth of frond-like clinopyroxene grains, chlorite, amphibole, dusty opaque minerals, and plagioclase. Clinopyroxene grains, and quenched skeletal plagioclase crystals such as have been described by Bryan (1972) and by Gélinas & Brooks (1974), occur as phenocrysts.

The effects of regional metamorphism are more conspicuous in tholeiites than in basaltic komatiites. Minerals such as prehnite, pumpellyite, carbonate, and chlorite fill fractures, veins, and cavities, and replace primary minerals such as plagioclase and pyroxene.

LAYERED FLOWS

Thick, layered peridotite–gabbro flows of both magma series are interlayered with the thinner flows. Two typical examples, one komatiitic and the other tholeiitic, have been described in detail by Arndt (1975, 1977). Mention of them is made here because they are important to our understanding of the nature of the komatiitic series. By comparing the characteristics of a particular section of the komatiitic layered flow with those of an analogous section of the tholeiitic layered flow, the distinguishing features of the two series defined through study of the thinner flows can be confirmed, and the compositional range over which these features apply is extended. Also, the komatiitic layered flow provides definitive evidence for the extent of differentiation of komatiitic magmas, and for the consanguinity of komatiitic basalts with the ultramafic lava types.

The principal features of two examples of layered flows are summarized in Figs. 15 to 18. The best example of a thick, layered flow of the komatiitic series, Fred's Flow (Figs. 15 and 16), has a maximum thickness of 120 m and has been traced a distance of over 3 km. This flow has a flowtop breccia of MgO-rich pyroxenitic komatiite (19·6 per cent MgO) made up of fragments and cobbles (1–10 cm) consisting for the most part of olivine phenocrysts set in a matrix of clinopyroxene and former glass. Toward the base of the breccia zone, individual fragments and matrix acquire a spinifex texture, and the rock grades in the massive spinifex-textured zone of the flow. The uppermost spinifex texture contains randomly-oriented wafers of olivine and resembles the spinifex texture found in olivine-poor peridotitic komatiite flows. The lower parts contain no olivine and are made up of parallel clinopyroxene needles of the type seen within some pyroxenitic and basaltic komatiites. There is a gradual but pronounced change in composition, from pyroxenitic to basaltic komatiite, from the flowtop breccia to the base of the spinifex zone (see Fig. 16).

Downloaded from https://academic.oup.com/petrology/article-abstract/18/2/319/1565696 by University of California, San Diego Library user on 28 March 2019

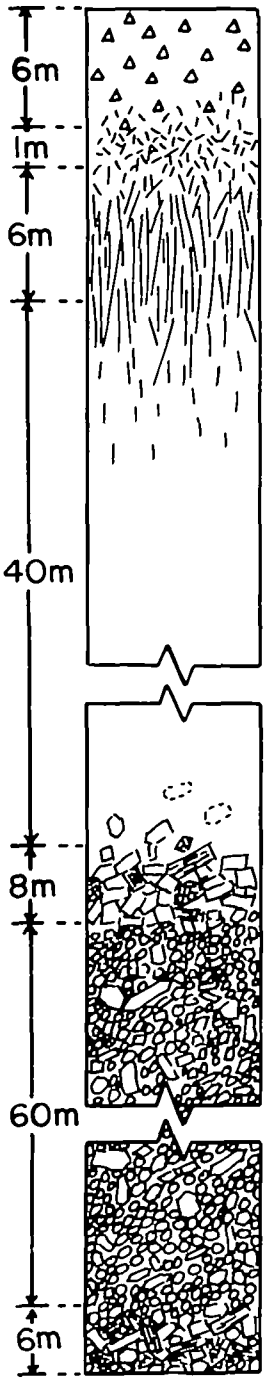

Flowtop breccia Fragments composed of 30% equant olivine phenocrysts in a matrix of clinopyroxene and devitrified glass.

Olivine spinifex textured lava 5% randomly oriented olivine wafers in a clinopyroxene-rich matrix.

Clinopyroxene spinifex textured lava Large needles of clinopyroxene with orthopyroxene or pigeonite cores oriented perpendicular to the flowtop, in a matrix of plagioclase and fine acicular pyroxene.

Transition zone Isolated large clinopyroxene grains in a basaltic matrix.

Medium-grained gabbro Discrete coarse grains of clinopyroxene and plagioclase. Up to 10% quartz in the groundmass.

Pyroxene cumulate Subhedral cumulate grains of clinopyroxene and lesser orthopyroxene.

Olivine cumulate Close-packed, equant, euhedral grains of olivine, minor anhedral and acicular clinopyroxene in a glassy groundmass.

Border zone 30% olivine, 30% orthopyroxene, 30% clinopyroxene; subhedral equant grains.

FIG. 15. Diagrammatic section through Fred's Flow—a komatiitic layered flow.

Downloaded from https://academic.oup.com/petrology/article-abstract/18/2/319/1565696 by University of California, San Diego Library user on 28 March 2019

The gabbro that underlies the spinifex zone has a medium-grained diabasic or equigranular texture. It is underlain by a thin interval of cumulate pyroxenites some of which are dominated by orthopyroxene, others by clinopyroxene. Rhythmic alternation of the two pyroxenes, and lower in the flow, of olivine, is a common feature of this zone. The thick cumulate peridotite zone has a more uniform composition and is composed of equant or, more rarely, elongate euhedral olivine grains in a matrix of acicular clinopyroxene, accessory brown basaltic hornblende (<2 per cent), chromite, and devitrified glass. The border zone contains equal proportions of equant euhedral grains of orthopyroxene, clinopyroxene, and olivine.

The presence of spinifex texture, the predominance of olivine cumulates, and the relative insignificance of pyroxene cumulates indicate the komatiitic affinity of this unit.

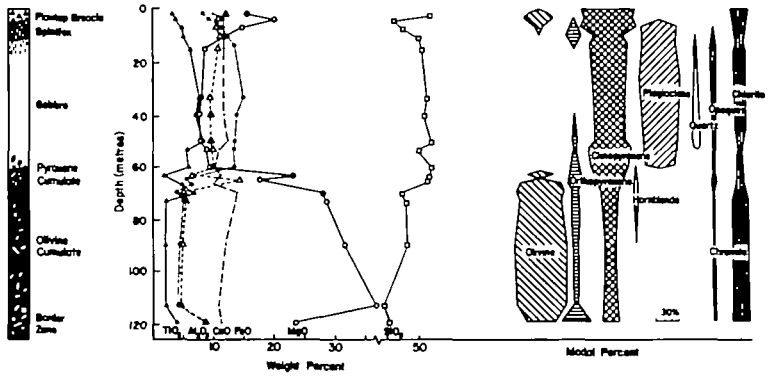

FIG. 16. Variation of dominant oxides and mineral phases in Fred's Flow (TiO_2 scale is enlarged ten times).

In contrast, the best example of a thick, layered flow of the tholeiitic series, Theo's Flow (Figs. 17 and 18), contains no spinifex texture, has a relatively thin cumulate olivine zone and is dominated by cumulate clinopyroxene. The flow is as thick as Fred's Flow but changes along strike from a sill intruding basalt flows, to a thick, layered flow, and then to a number of thinner flows of basalt lava or fragmental material (Arndt, 1975). In the thick, layered section, the flowtop zones consist of coarse and fine hyaloclastite breccias of pyroxenitic or picritic compositions (ca. 14 per cent MgO). These are underlain by aphanitic pyroxenite, also of highly mafic composition (12 per cent MgO), beneath which is medium-grained gabbro, cumulate pyroxenite, and a thin basal veneer of cumulate perioditite.

KOMATIITIC AND THOLEIITIC INTRUSIONS

Intrusive equivalents of the extrusive lavas occur in Munro and adjacent townships.

Peridotite sills. Several small sills or dikes (5–50 m thick) that are mineralogic-

Downloaded from https://academic.oup.com/petrology/article-abstract/18/2/319/1565696 by University of California, San Diego Library user on 28 March 2019

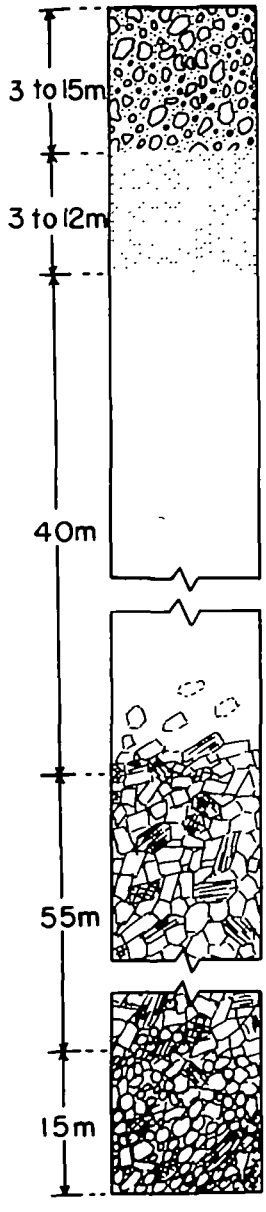

Hyaloclastite Well-sorted, pea-sized fragments, or larger angular fragments and globules of glassy pyroxenitic material.

Aphanitic pyroxenite Fine pyroxene grains mantled by brown amphibole.

Pegmatoid gebbro Patchy distribution of coarse to very coarse (3 cm) subhedral grains of clinopyroxene and plagioclase.

Normal gabbro Medium grained clinopyroxene and plagioclase.

Noritic gabbro 10% orthopyroxene grains, now altered to chlorite, within a normal gabbroic rock.

Pyroxene cumulate Subhedral grains of clinipyroxene and lesser, (10%) orthopyroxene.

Olivine cumulate 70% equant subhedral grains of olivine, 20% anhedral grains of clinopyroxene and orthopyroxene in a glassy matrix.

FIG. 17. Diagrammatic sections through Theo's Flow—a tholeiitic layered flow.

ally and chemically similar to peridotitic komatiite lavas, intrude the volcanic succession. Most sills contain a central zone of close-packed equant olivine phenocrysts in a clinopyroxene and devitrified glass matrix, and marginal zones of the same mineralogy but poorer in olivine. They may be feeders to ultramafic komatiite lava flows.

Layered peridotite–gabbro sills. Layered sills of the Munro region have been

Downloaded from https://academic.oup.com/petrology/article-abstract/18/2/319/1565696 by University of California, San Diego Library user on 28 March 2019

described previously by Satterly (1951), Naldrett & Mason (1968), MacRae (1969), and Arndt (1975). They may be similar in dimensions to the layered flows or may be much larger. The Munro–Warden sill is more than 1000 m thick and has a strike length of more than 6 km.

Sills of both magma series have been recognized on the basis of their petrology, which generally is similar to that of their extrusive analogues. However, in the thicker intrusions grainsize is larger, and the dimensions of individual layers is greater. As with the layered flows, sills of tholeiitic affinity are characterized by a predominance of clinopyroxene-rich cumulates over olivine cumulates

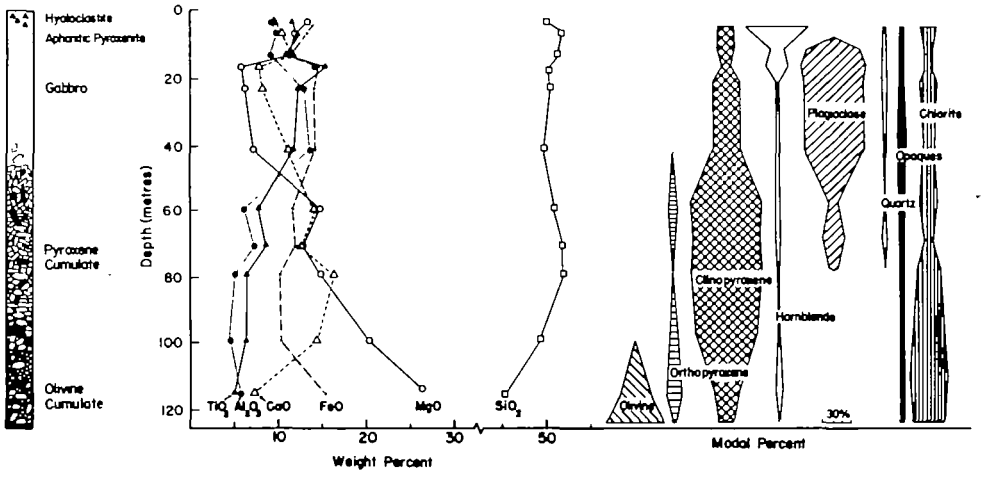

FIG. 18. Variation of dominant oxides and mineral phases in Theo's Flow. (TiO_2 scale is enlarged ten times.)

(*e.g.* the Munro–Warden Sill; MacRae, 1969, or the Dundonald Sill; Naldrett & Mason, 1968), whereas komatiitic examples contain a larger proportion of cumulate olivine, a smaller proportion of cumulate pyroxene, and minor disseminated sulphide mineralization (the Munro–Beatty Sill; MacRae, 1969; Arndt, 1975).

CHEMISTRY

Table 7 contains analyses of typical komatiitic and tholeiitic lavas, as well as average compositions of the main classes of komatiite and the average composition of tholeiitic basalts in Munro Township. On file at the National Research Council of Canada, Ottawa, are more than 200 additional analyses.

Major elements, except Na_2O, were analysed at University of Toronto with a Philips PW 1540 X-ray spectrometer, using analytical techniques similar to those of Norrish & Chappel (1967), and the international rock standards BCR-1 (basalt) and P-1-24 (picrite). Na_2O was determined by atomic absorption, and S with a Leco Induction Furnace and Automatic Titrator. Values listed are

Downloaded from https://academic.oup.com/petrology/article-abstract/18/2/319/1565696 by University of California, San Diego Library user on 28 March 2019

TABLE

Representative analyses of komatiites

	1	2	3	4	5	6	7	8	9
SiO_2	40·0 (44·0)*	41 2 (44·2)	41·4 (44·4)	44·2 (45·6)	41·1 (43·5)	42·2 (45 9)	45·6 (48·2)	44·9	46·0
TiO_2	0·14 (0·15)	0·17 (0·18)	0·33 (0·35)	0·26 (0·27)	0·42 (0·44)	0·28 (0·30)	0·46 (0·49)	0·19	0·32
Al_2O_3	3·70 (4·1)	4·84 (5·02)	6·90 (7·40)	7·12 (7·35)	8·74 (9·24)	6·10 (6·663)	8·40 (8·89)	5·3	7·4
Cr_2O_3	0·26 (0·28)	n.d.	0·45 (0·47)	0·40 (0·41)	0·48 (0·49)	0·30 (0·32)	0·29 (0·31)	0·26	0·39
Fe_2O_3 FeO	8·2 (9·0)	10·1 (10·4)	12·4 (13·3)	11·3 (11·7)	12·8 (13·5)	10·5 (11·4)	2·46 (2·63) 8·2 (8·7)	10·4	11·5
MnO	0·15 (0·16)	0·20 (0·21)	0·24 (0·26)	0·20 (0·21)	0·20 (0·21)	0·22 (0·24)	0·19 (0·20)	0·18	0·22
MgO	35·1 (38·6)	32·1 (34·5)	25·6 (27·5)	25·1 (25·9)	22·1 (23·4)	26·3 (28·6)	20 6 (21·8)	33·6	26·5
NiO	0·03 (0·03)	0·21 (0 23)	0 02 (0 02)	0·16 (0·17)	0·01 (0·01)	0·02 (0·02)	0·01 (0·01)	0·02	0·01
CaO	3·28 (3·61)	4·04 (4·34)	5·90 (6.33)	7·39 (7.62)	8·76 (9·26)	5·83 (6.34)	8·1 (8·6)	5·0	7·4
Na_2O	0·07 (0·08)	0·28 (0·30)	0·06 (0 06)	0·80 (0·83)	0·11 (0·12)	0·19 (0·21)	0·46 (0·49)	0·35	0·45
K_2O	0·10 (0·11)	0·02 (0·02)	0·07 (0·08)	0·06 (0·06)	0·01 (0·01)	0 11 (0·12)	0·03 (0·03)	0·08	0·10
H_2O^+							(4·08)		
LOI H_2O^-	9·3	6·9	7·4	3·1	6·2	7·8	5·2 0·77		
CO_2							0·36		
TOTAL	100·3	100·1	100·8	100·1	100·9	99·9	100·0		
S	—	—	0·04	—	—	0·08	0·04		
Cr	1762	—	3080	—	3272	2263	2009		
Co	118	—	122	—	109	118	93		
Ni	2290	—	1470	—	980	1706	986		
Zn	54	—	101	—	80	73	80		
Rb	3	—	3	—	2	7	5		
Sr	6	—	3	—	6	22	15		
Q	0·0	0·0	0·0	0 0	0·0	0·0	0·0		
Or	0·6	0·12	0·43	0·35	0·18	0·67	0·18		
Ab	0·6	2·50	0·55	7·09	4·25	1·76	4·25		
An	9·6	11·85	18·9	15·46	21·36	15·98	21·36		
Ne	0·0	0·0	0·0	0·0	0·0	0·0	0·0		
Cpx	5·4	6·50	9·0	16·59	15·97	11·12	15·97		
Opx	12·3	13·11	19·3	8·53	30·25	21·65	30·25		
Ol	71·3	65·68	51·4	51·61	27·33	48·41	27·33		
Il	0·2	0·24	0·47	0·36	0·66	0·40	0·66		
Mg/Mg+Fe	0·88	0·85	0·79	0·80	0·76	0·82	0·80		

Notes.
LOI—Loss on ignition. n.d.—not determined.
* Anhydrous values. Oxides and S expressed in weight percent; trace elements in ppm.
1. P9-119—Cumulate peridotite from B-zone of peridotitic komatiite flow.
2. SA-2039—Cumulate peridotite from B-zone of peridotitic komatiite flow.
3. P9-118—Spinifex-textured peridotitic komatiite.
4. SA-2048—Spinifex-textured peridotitic komatiite.
5. P9-120—Flowtop (A_1-zone), spinifex-textured peridotitic komatiite flow.
6. P9-116—Spinifex-free peridotitic komatiite lava.
7. P9-130—Spinifex-free peridotitic komatiite lava.

Downloaded from https://academic.oup.com/petrology/article-abstract/18/2/319/1565696 by University of California, San Diego Library user on 28 March 2019

7

and tholeiites in Munro Township

10	*11*	*12*	*13*	*14*	*15*	*16*	*17*	*18*	
48·3 (50·4)	47·2 (49·5)	50·2	50·4 (52·2)	51·2 (53·0)	51·6	50·4 (51·7)	48·6 (50·9)	51·1	SiO_2
0·62 (0·65)	0·43 (0·45)	0·61	0·57 (0·59)	0·80 (0·83)	0·65	1·39 (1·43)	1·51 (1·58)	1·70	TiO_2
10·8 (11·3)	11·9 (12·5)	11·6	12·0 (12·3)	13·9 (14·4)	13·3	12·6 (12·8)	12·0 (12·6)	13·3	Al_2O_3
0·21 (0·23)	n.d.		0·02 (0·02)	0·03 (0·03)		0·01 (0·01)	0·03 (0·03)		Cr_2O_3
2·35 (2·46)	1·79 (1·88)	11·11	1·90 (1·97)	2·58 (2·67)	11·7	13·9 (14·3)	2·80 (2·93)	15·0	Fe_2O_3
7·4 (7·7)	9·5 (10·0)		9·4 (9·8)	8·2 (8·49)			12·0 (12·6)		FeO
0·18 (0·19)	0·20 (0·21)	0·19	0·17 (0·18)	0·17 (0·18)	0·19	0·24 (0·25)	0·21 (0·22)	0·28	MnO
13·9 (14·4)	12·6 (13·2)	14·3	10·2 (10·6)	7·50 (7·76)	10·0	5·11 (5·24)	4·67 (4·89)	5·92	MgO
0·01 (0·01)	n.d.		0·0 (0·0)	0·0 (0·0)		0·0 (0·0)	0·0 (0·0)		NiO
10·0 (10·5)	9·9 (10·4)	9·6	11·1 (11·5)	10·8 (11·2)	10·4	11·9 (12·2)	9·40 (9·84)	8·6	CaO
2·24 (2·34)	1·91 (2·01)	2·34	0·56 (0·58)	1·77 (1·83)	2·16	1·21 (1·24)	4·60 (4·81)	3·9	Na_2O
0·00 (0·00)	0·01 (0·01)	0·05	0·28 (0·29)	0·02 (0·02)	0·11	0·77 (0·79)	0·05 (0·05)	0·25	K_2O
2·77	3·3		2·89	3·2			2·67		H_2O^+
3·9 0·31	3·9 0·41		3·3 0·24	3·5 0·18		2·3	4·3 0·26		LOI H_2O^-
0·74	0·02		0 20	0·10			1·37		CO_2
99·9	99·3		99·9	100·5		99·8	100·2		TOTAL
0 02	0·32		0·12	0·10		0·10	0·27		S
1460	—		143	227		82	209		Cr
80	—		66	46·8		70	346		Co
647	—		93	89		67	99		Ni
n.d.	—		79	n.d.		125	n.d.		Zn
1	0·2		8	2		13	1		Rb
41	75		97	94		130	67		Sr
0 0	0 0		3 52	3·19		3·44	0·0		Q
0·0	0·06		1·74	0·12		4·83	0·31		Or
20·61	17·78		5·27	16·61		11·52	34·31		Ab
19·90	24·76		30·85	31·28		28·29	12·63		An
0·0	0·0		0·0	0·0		0·0	5·59		Ne
24·76	20·95		21·54	19·78		27·46	29·32		Cpx
11·12	13·87		36·25	27·86		22·41	0·0		Opx
22·73	21·95		0·0	0·0		0·0	15·61		Ol
0·89	0·62		0·83	1·16		2·05	2·2		Il
0·72	0·67		0·63	0·57		0·40	0·36		Mg/Mg+Fe

8. Average composition of peridotitic komatiites with MgO > 30%.
9. Average composition of peridotitic komatiites with MgO < 30%.
10. P9-132—Olivine-rich pyroxenitic komatiite lava.
11. P9-185—Pyroxene-rich pyroxenitic komatiite lava.
12. Average composition of pyroxenitic komatiites.
13. P9-108—Basaltic komatiite lava.
14. P9-13—Basaltic komatiite lava.
15. Average composition of basaltic komatiites.
16. P9-101—Tholeiitic basalt.
17. P9-195—Tholeiitic basalt.
18. Average composition of tholeiitic basalts.

Downloaded from https://academic.oup.com/petrology/article-abstract/18/2/319/1565696 by University of California, San Diego Library user on 28 March 2019

averages of at least two replicate analyses. Maximum errors are estimated at 2 to 3 per cent of the amount present for SiO_2, TiO_2, Al_2O_3, and MnO; 1 to 2 per cent for total iron, MgO, Na_2O, and CaO; and 3 to 5 per cent for K_2O.

Trace elements were analysed at Université de Montréal using techniques described by Watkins, Gunn & Coy-yll (1970).

Chemical compositions of komatiites

The most ultramafic komatiites are basal cumulates of peridotitic komatiite flows (P9-119 and SA 2039). These rocks have ultrabasic ($SiO_2 < 45$ per cent) compositions with high MgO contents (MgO > 30 per cent), and low CaO,

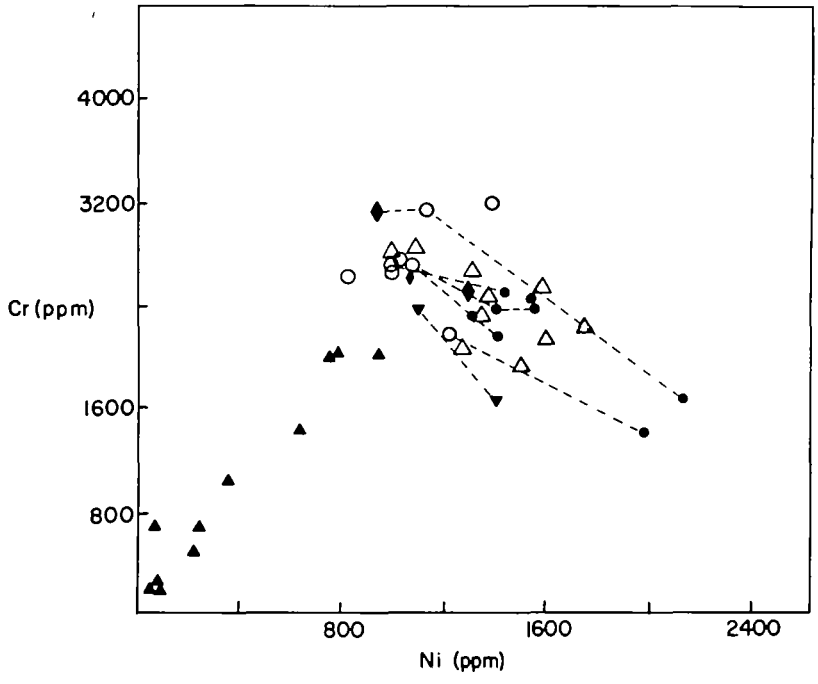

FIG. 19. Cr *vs.* Ni diagram for komatiitic lavas. *Dashed lines* connect units of the same flow. Symbols: *diamonds*—flowtop, peridotitic komatiite flow; *open circle*—spinifex-textured lava; *solid circle*—cumulate zone; *open triangle*—spinifex-free peridotitic komatiite lava; *solid triangle*—other komatiitic lavas; *inverted triangle*—centre and margin of peridotitic komatiite sill.

Al_2O_3, TiO_2, and alkalis. Less mafic peridotitic komatiites include spinifex-textured rocks that are thought to represent liquid lavas (P9-118), and massive porphyritic lavas (P9-116). Their compositions also are ultrabasic. Pyroxenitic and basaltic komatiites have basic compositions with proportionately lower MgO, NiO, and Cr_2O_3 contents and higher CaO, Al_2O_3, SiO_2, and TiO_2 contents.

As the mafic mineral content of komatiitic lavas decreases, MgO and NiO steadily decrease and CaO, Al_2O_3, SiO_2, and TiO_2 steadily increase. Na_2O, K_2O, Rb, and Sr also increase, but their trends have been complicated by migra-

Downloaded from https://academic.oup.com/petrology/article-abstract/18/2/319/1565696 by University of California, San Diego Library user on 28 March 2019

tion of these elements during alteration. Total iron and MnO increase slightly but in an irregular manner. Cr_2O_3 values are low in cumulus peridotitic komatiites, increase rapidly to a maximum in spinifex-textured peridotitic komatiites (MgO ≈ 25 per cent, Ni ≈ 1100 ppm) and then decrease as MgO decreases in pyroxenitic and basaltic komatiites (Fig. 19). This behaviour results from the relatively late stage at which chromite starts to crystallize, a stage following the crystallization of much olivine and the formation of cumulus peridotitic komatiites.

The main chemical variations are well illustrated on the MgO–CaO–Al_2O_3 (MCA) diagram of the type used by Viljoen & Viljoen (1969*a*) and Nesbitt (1971) (Fig. 20). The trend in peridotitic and pyroxenitic komatiite compositions

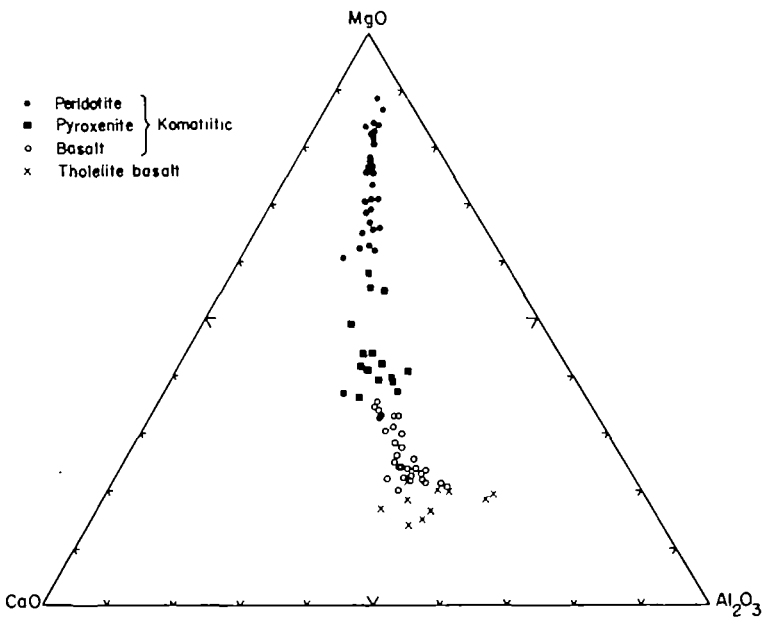

FIG. 20. MgO–CaO–Al_2O_3 diagram showing composition of komatiitic and tholeiitic lavas of Munro Township.

is essentially one of decreasing MgO at constant CaO/Al_2O_3 ratio, reflecting the importance of olivine fractionation. Olivine removal is the dominant control through to basaltic komatiite compositions, at which stage clinopyroxene, and finally plagioclase fractionation become important. Removal of clinopyroxene is responsible for the curvature towards the MgO–CaO side of the diagram. The slight curvature towards the MgO–CaO side of the diagram near the MgO apex reflects preferential loss of CaO during serpentinization.

The interpretation of the Munro komatiites as a fractionation sequence is consistent with what would be predicted by phase relationships in simple systems. In Fig. 21 the average composition of 5 groups of rocks representing

Downloaded from https://academic.oup.com/petrology/article-abstract/18/2/319/1565696 by University of California, San Diego Library user on 28 March 2019

komatiitic liquids are projected into the $Ca_{0.5}(MgFe)_{0.5}O$–$(MgFe)O$–SiO_2 mole per cent diagram as outlined by Irvine (1970). The phase relations shown are those for the diopside–forsterite–silica system after Kushiro (1969), and do not apply directly to the iron-bearing system. In the diagram, it has been assumed that the initial lava composition (1) is the average composition of the spinifex zone of the flow sampled by drilling on Pyke Hill. Succeeding liquids are taken

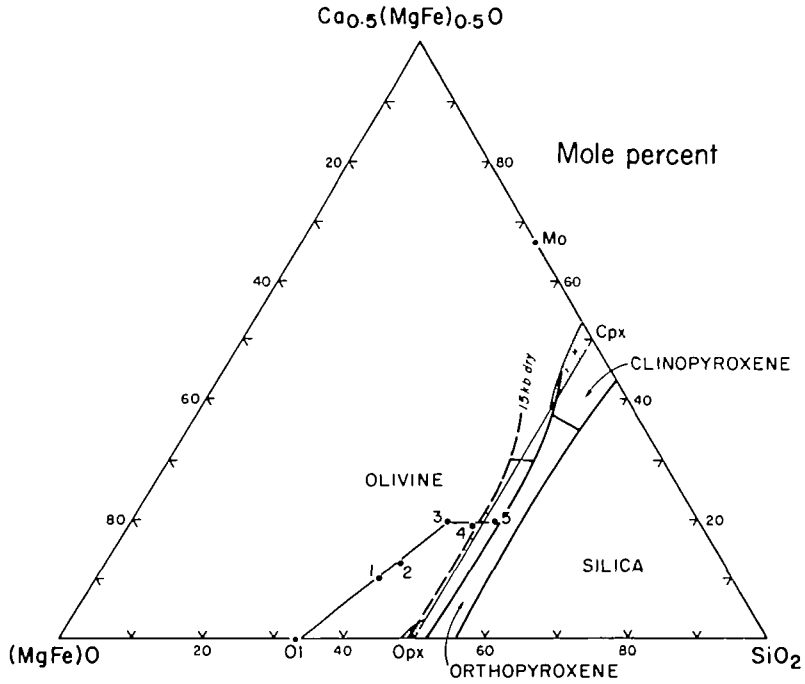

FIG. 21. $Ca_{0.5}(MgFe)_{0.5}O$–$(MgFe)O$–SiO_2 mole per cent diagram (after Irvine, 1970) showing average cationic normative compositions of five groups of komatiitic rocks representative of silicate liquids.

as (2) the average composition of all spinifex-textured rocks with 20–25 per cent MgO; (3) spinifex-textured pyroxenitic komatiites with 12–20 per cent MgO; (4) basaltic komatiites with 10–12 per cent MgO; and (5) basaltic komatiites with less than 10 per cent MgO. Liquids 1–3 fall on a line of olivine control, whereas the path from 3 to 5 apparently requires co-precipitation of both olivine and clinopyroxene.

In Fig. 22 analyses of komatiitic lavas are plotted in diagrams that are commonly used to discriminate between various magma types. With the exception of certain altered samples that have become enriched in alkali elements, the komatiites fall well within the fields normally assigned to tholeiitic magmas.

In contrast with other geologists working with komatiites who include in the association only those rocks with MgO values greater than 9–12 per cent (*e.g.* Brooks & Hart, 1974), we have included basalts with values of 8 per cent or less. Our justification is based in part on field data, particularly the close spatial

Downloaded from https://academic.oup.com/petrology/article-abstract/18/2/319/1565696 by University of California, San Diego Library user on 28 March 2019

relationship between the least mafic and the ultramafic types of komatiite and the progressive change from perioditite to basaltic compositions within a single volcanic cycle (Fig. 5). Other features considered important are the common presence of spinifex texture in all types of komatiitic lavas including basalts, the continuous spread of data in the MCA diagram (Fig. 20), and the similarity between the composition of the devitrified glass matrix of peridotitic komatiite

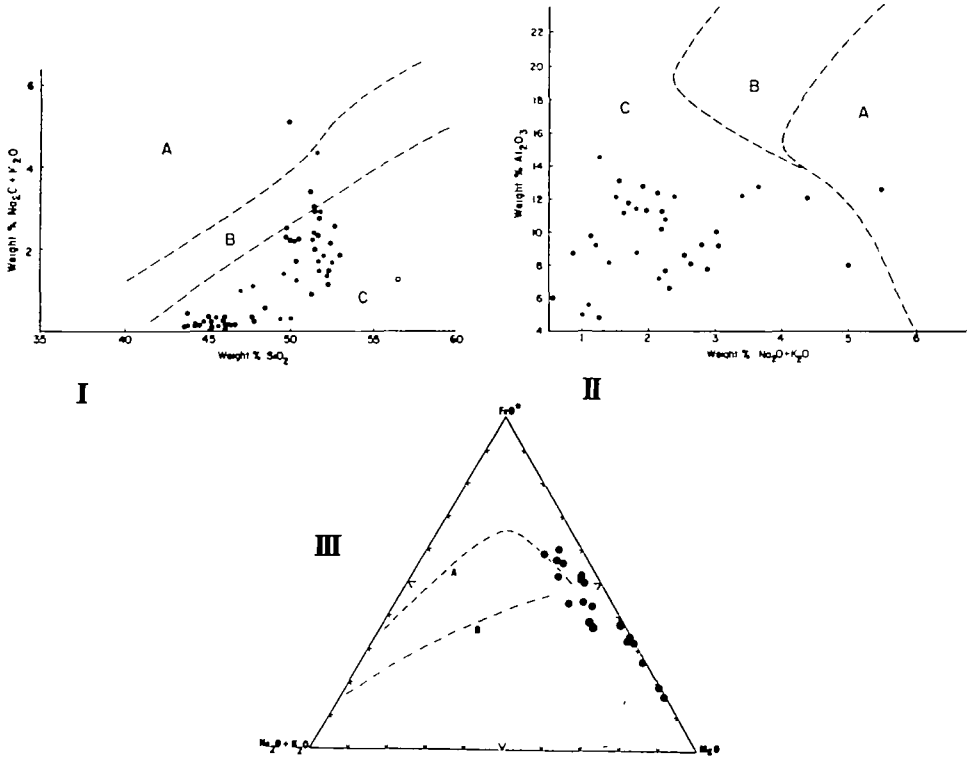

FIG. 22. Variation diagrams comparing the compositions of komatiitic lavas with compositional fields of other magma series. Fields in diagrams I and II: A—alkali basalts; B—high alumina basalts; C—tholeiitic basalts (after Kuno, 1966). In diagram III trend A represents tholeiitic lavas from the Thingmuli volcano (Carmichael, 1964); trend B represents calc-alkaline lavas from the Cascades (Nockolds & Allen, 1956).

lavas, and the whole-rock compositions of pyroxenitic and basaltic komatiite lavas (Tables 5 and 7). The best evidence, however, comes from the thick, layered komatiitic flow, in which the gabbroic portion, which has gradational contacts with overlying ultramafic flowtop zones, has a MgO-poor composition identical to many basaltic komatiite lavas.

Chemical characteristics of tholeiitic rocks from Munro Township

Tholeiitic volcanic rocks from Munro Township range in composition from picrite to dacite, but most are basalts with compositions similar to the average listed in Table 7. This composition represents a type of iron-rich and TiO_2-rich

Downloaded from https://academic.oup.com/petrology/article-abstract/18/2/319/1565696 by University of California, San Diego Library user on 28 March 2019

tholeiite apparently common in Archean areas (Pearce & Birkett, 1974; Naldrett & Goodwin, 1977; Naldrett & Turner, 1977). The tholeiitic thick, layered flows and sills have gabbroic units of similar composition to the tholeiitic basalts, but are capped by picritic hyaloclastitites, and are underlain by pyroxenitic and peridotitic cumulates.

Comparison of komatiites and tholeiites in Munro Township

T. N. Irvine (pers. comm. 1971) pointed out that the Al_2O_3 *vs.* FeO*/(FeO*+MgO) plot (Fig. 23) separated rocks such as the 'overlying lenses', a sequence of rocks described by Naldrett & Mason (1968) that are now regarded as komatiitic lavas, from differentiated tholeiitic sills such as the Dundonald Sill (Nal-

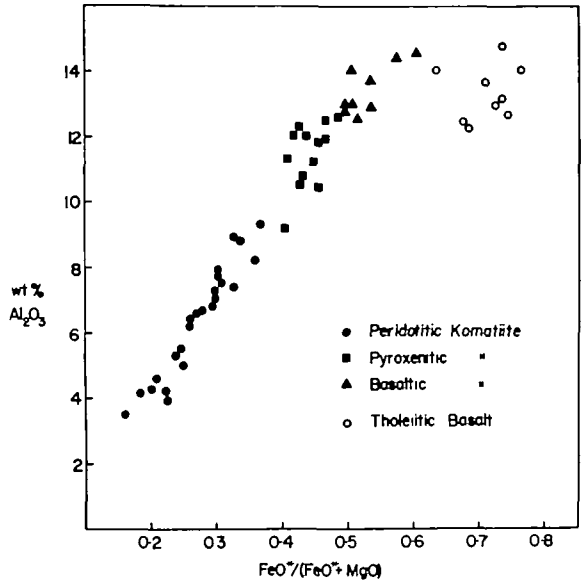

FIG. 23. Al_2O_3 *vs.* FeO*/(FeO*−MgO) diagram showing compositions of komatiitic and tholeiitic lavas.

drett & Mason, 1968) and the Munro–Warden Complex (MacRae, 1969). The diagram is most useful in distinguishing komatiites from tholeiites at Munro (Figs. 23 and 24). Komatiites consistently have lower FeO*/(FeO*+MgO) ratios than tholeiites of similar Al_2O_3 content. This relationship is true for both noncumulate and cumulate rocks, and holds not only for mafic rocks in which there is a large degree of compositional overlap between tholeiites and komatiites, but also for the entire range in composition of the thick, layered flows and sills. Komatiites with low Al_2O_3 contents such as those from the Barberton Mountain Land fall in the tholeiitic field in this diagram. These rocks are distinguishable from tholeiites by their high CaO/Al_2O_3 ratios.

Figures 25 and 26 illustrate a second feature that discriminates between rocks

Downloaded from https://academic.oup.com/petrology/article-abstract/18/2/319/1565696 by University of California, San Diego Library user on 28 March 2019

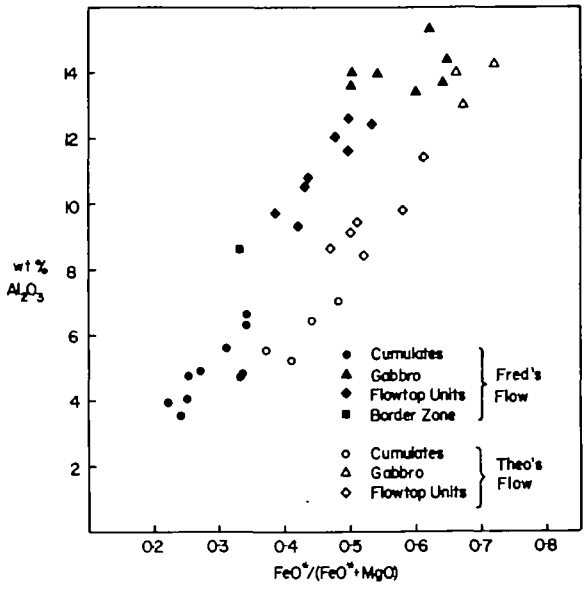

FIG. 24. Al_2O_3 *vs.* $FeO^*/(FeO^*-MgO)$ diagram showing compositions of layered flows.

of the two series. For any composition, which may be specified by MgO or SiO_2 content, the TiO_2 content of a tholeiitic rock exceeds that of a komatiite (cf. Brooks & Hart, 1974). This relationship also holds both for the discrete lava flows and for the thicker layered flows.

Of lesser importance are MgO, NiO, and Cr_2O_3, which are generally high in komatiites, and the alkalis, Al_2O_3 and FeO^*, which are low.

The ratio CaO/Al_2O_3, which Viljoen & Viljoen (1969*a*, *b*) considered the most distinctive feature of the komatiites from Barberton Mountain Land, is not

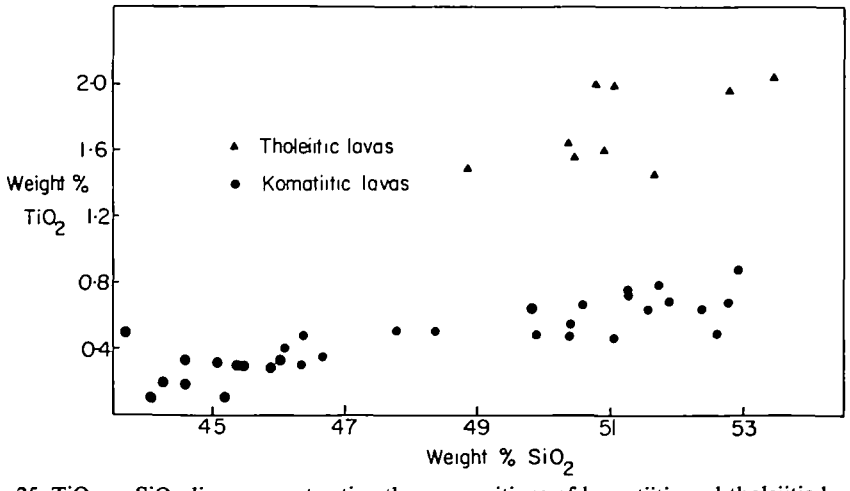

FIG. 25. TiO_2 *vs.* SiO_2 diagram contrasting the compositions of komatiitic and tholeiitic lavas.

Downloaded from https://academic.oup.com/petrology/article-abstract/18/2/319/1565696 by University of California, San Diego Library user on 28 March 2019

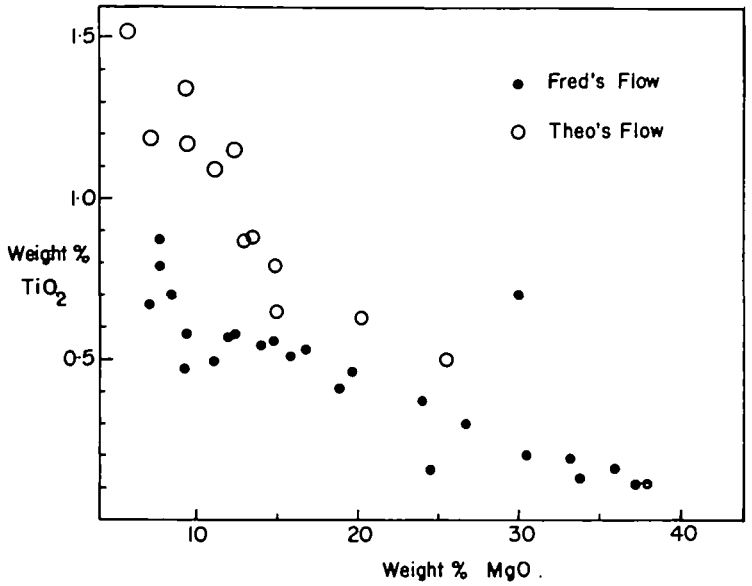

FIG. 26. TiO_2 *vs.* MgO diagram showing compositions of layered flows.

diagnostic in Munro. Although CaO/Al_2O_3 ratios of basaltic komatiites generally exceed those of tholeiitic basalts, this difference is a reflection of the less mafic composition of the tholeiites. Figure 27 shows that a komatiite from Munro Township cannot be distinguished from a tholeiite of similar MgO content by CaO/Al_2O_3 ratio.

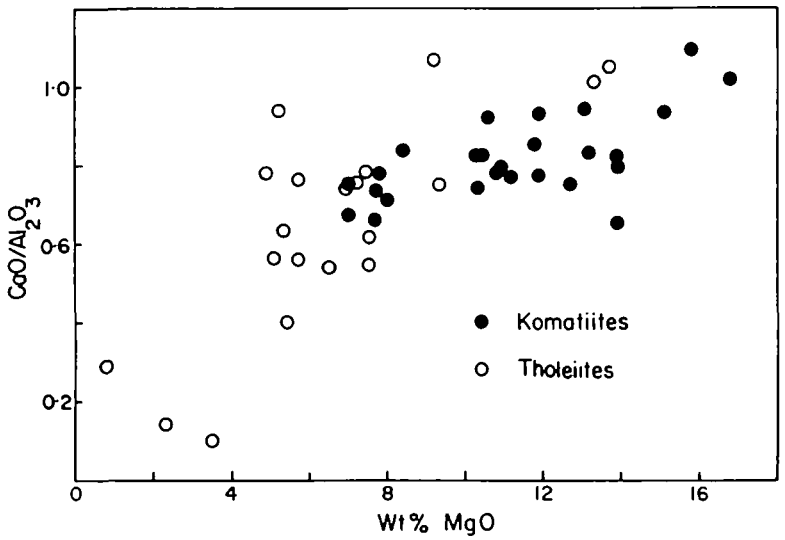

FIG. 27. CaO/Al_2O_3 *vs.* MgO diagram showing the similarity between komatiites and tholeiites in Munro Township.

Downloaded from https://academic.oup.com/petrology/article-abstract/18/2/319/1565696 by University of California, San Diego Library user on 28 March 2019

TABLE 8

Comparison of characteristics of komatiites and tholeiites of Munro Township

		Field	*Petrologic and Mineralogic*	*Chemical*
Komatiites	Ultramafic	Dark gray to black heavy, magnetic lava rich in olivine; may contain spinifex texture or polyhedral jointing. Cumulate and non-cumulate types are common.	Rich in very forsteritic, chrome-rich olivine (Fo_{88-94}) as equant solid, or skeletal grains; aluminous sub-calcic pyroxenes as skeletal grains; magnesium-rich devitrified glass groundmass.	Low FeO*/(FeO*+MgO) and TiO_2; very high MgO, NiO, Cr_2O_3.
	Mafic	Pale gray-green, hard, relatively coarse-grained lava; may contain lava toes or clinopyroxene spinifex texture.	Skeletal or equant grains of aluminous sub-calcic pyroxene, commonly intergrown with calcic plagioclase.	Low FeO*/(FeO*+MgO)(<0·65), low TiO_2 (<1·0%), low alkali elements; moderately low Al_2O_3; high MgO, Cr_2O_3, NiO
Tholeiites	Ultramafic	No non-cumulate olivine-rich rocks. Pyroxenite occurs as hyaloclastite flow tops of thick layered flows, and as cumulate rocks in flows and sills.	Cumulates are composed of combinations of olivine (Fo_{88-82}), orthopyroxene and clinopyroxene. Non-cumulate rocks are fragmental, largely glassy, with phenocrysts of olivine, clinopyroxene and plagioclase.	Relatively high (FeO*/(FeO*+MgO), and high TiO_2.
	Mafic	Pillowed, massive or fragmental lava; dark gray-green, finer and more highly altered than basaltic komatiites.	Fine grained equigranular or porphyritic lava; may contain phenocrysts of clinopyroxene or plagioclase; skeletal plagioclase grains in chilled samples; rich in very fine grained iron oxides.	Relatively high FeO*/(FeO*+MgO), TiO_2 and FeO*; low MgO, Cr_2O_3, NiO.

SUMMARY OF DISTINCTIVE FEATURES OF KOMATIITES AND THOLEIITES

Field, petrologic, and chemical features by which a Munro komatiite can be distinguished from a tholeiite are summarized in Table 8. The range in composition of rocks representing komatiitic liquids is from peridotite to andesite (28–12 per cent MgO, 44–56 per cent SiO_2), whereas that of rocks representing tholeiitic liquids is from picrite to dacite (15–<2 per cent MgO, 48–>65 per cent SiO_2). Thus any rock containing more than 15 per cent MgO that can be shown by textural or other evidence to be noncumulate probably belongs to the komatiitic series. Furthermore, in Munro Township, noncumulate picritic tholeiites are only found in the flowtops and chilled margins of thick, differentiated flows and sills, and any noncumulate, nondifferentiated volcanic rock more mafic than a basalt is likely to be komatiitic.

The most useful textural feature that distinguishes a rock as komatiitic is spinifex texture, either the olivine-dominated type, described by Nesbitt (1971), or the clinopyroxene-dominated type that forms the tops of pyroxenitic komatiite flows. Spinifex texture is easily recognized in outcrop and hand specimen and commonly survives relatively high grades of metamorphism and structural deformation. Also useful are polyhedra and crescent-shaped schlieren in peridotitic and pyroxenitic komatiite flows. Grain size, which tends to be coarser in komatiites than tholeiites, degree of alteration, which tends to be lower in komatiites, and lava colour may also be helpful in areas of low metamorphic grade but tend to be obliterated at higher grades.

Downloaded from https://academic.oup.com/petrology/article-abstract/18/2/319/1565696 by University of California, San Diego Library user on 28 March 2019

The chemical parameters, $FeO^*/(FeO^*+MgO)$ at a given Al_2O_3 content, and TiO_2 value at a given SiO_2 or MgO content are the most reliable means of distinguishing between the two magma types.

COMPARISON OF MUNRO ROCKS WITH SIMILAR ROCKS FROM OTHER AREAS

Archean Komatiites. Ultramafic lavas and related rocks have been recognized in most Archean shield areas: in South Africa (Viljoen & Viljoen, 1969*a*, *b*); in Canada (Naldrett & Mason, 1968; Brooks & Hart, 1972, 1974; Eckstrand, 1972; Pyke *et al.* 1973; Gélinas & Brooks, 1974; Jolly, 1975; Shau, 1975); in Australia (McCall, 1971; Nesbitt, 1971; Williams, 1972; Lewis & Williams, 1973; Barnes *et al.* 1974; Naldrett & Turner, 1977); in Rhodesia (Anhaeusser, 1971; Bickle *et al.* 1975); and in India (Viswanathan, 1974). In some of these reports the ultramafic and mafic lavas are not called komatiites but are referred to by other names such as 'Archean peridotites' and 'high Mg basalts' (Williams, 1972) or 'magnesian lavas' (Jolly, 1975; Arndt, 1976*b*). Inspection of these reports indicates that rocks from all areas mentioned except Barberton Mountain Land have similar field characteristics, primary mineralogy, and chemical composition to the komatiites of Munro Township. CaO/Al_2O_3 ratios generally cluster about 1; in some samples a little higher but in most somewhat lower. High CaO/Al_2O_3 ratios, and, more specifically, ratios greater than 1 do not appear to be characteristic of the group as a whole, but $FeO^*/(FeO^*+MgO)$ ratios and TiO_2 contents are comparable to those in the Munro rocks (Figs. 27 and 28).

Tholeiitic and Other Archean Basalts. Iron-rich tholeiites like those in Munro Township are associated with komatiites in other areas. Naldrett & Turner (1977) point this out in the Yakabindie area of the Eastern Goldfields of Western Australia, demonstrating that the criteria developed for Munro adequately distinguish the majority of the tholeiites from komatiites. Inspection of analyses from Quebec (Gélinas & Brooks, 1974; Kretschmar & Kretschmar, 1975), the Kalgoorlie region of the Eastern Goldfields (Williams, 1972; Nesbitt, 1971), and the Barberton Mountain Land (Viljoen & Viljoen, 1969*c*) indicate that the criteria are also good discriminants in these areas.

However, basalts in parts of Archean greenstone belts removed from ultramafic komatiites, such as the major part of the Blake River Group (Goodwin, 1973) and the upper parts of stratigraphic cycles in the Kalgoorlie area (Gemuts & Theron, 1975) generally do not have such high FeO^* and TiO_2 contents. The averages of Archean basalt compositions of Goodwin (1968) and Hallberg (1972) have only slightly higher FeO^* and TiO_2 values than the average of basaltic komatiites in Munro Township. Jolly (1975) and Naldrett & Goodwin (1977) applied chemical screens to raw analytical data from the Blake River Group and showed that a certain proportion of analyses represent basalts of

Downloaded from https://academic.oup.com/petrology/article-abstract/18/2/319/1565696 by University of California, San Diego Library user on 28 March 2019

magma series other than the tholeiitic series. Naldrett & Goodwin recognized komatiitic basalts, iron-rich tholeiites, and Al-rich basalts (16–22 per cent Al_2O_3) and a large group of basalts transitional between these types that they were unable to assign to a particular category. Using the criteria outlined in this paper, they were able to distinguish as komatiitic few basalts with less

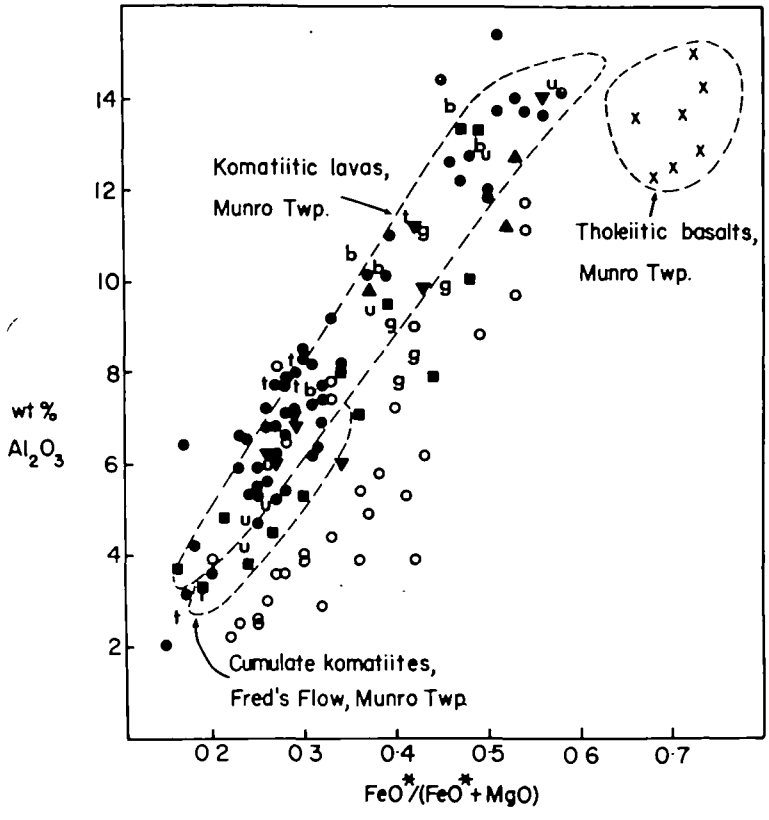

FIG. 28. Al_2O_3 *vs.* FeO*/FeO*+MgO) for komatiites from Canada (*squares*) (Brook & Hart, 1972; Naldrett & Mason, 1968; Gélinas & Brooks, 1974, and unpublished data); Australia (*filled circles*) (Williams, 1972; McCall, 1971; Nesbitt, 1971, Nesbitt & Sun, 1976; Barnes *et al.* 1974); India (*triangles*) (Viswanathan, 1974); Rhodesia (*inverted triangles*) (Bickle *et al.* 1975) and Barberton Mountain Land (*circles*) (Viljoen & Viljoen, 1969a). Also shown are Fe-rich tholeiites associated with komatiites (x) from Canada (Pearce & Birkett, 1974) and Australia (Williams, 1972): Proterozoic komatiites from Ungava, Canada (u) (Wilson *et al.* 1969) and Thompson, Manitoba (t) (Stephenson, 1974); Lower Palaeozoic komatiites from Rambler, Newfoundland (g) (Gale, 1973): and Tertiary picritic basalts from Baffin Bay (b) (Clark, 1970).

than 8·5 per cent MgO. It is our opinion that the application of the chemical criteria developed in Munro cannot provide a positive separation between all tholeiitic basalts and basaltic komatiites. Only in areas where the basalts are associated with ultramafic komatiites can the chemical criteria be applied with confidence. Where no such association exists, no conclusions can be drawn.

Younger Rocks. Rocks that share many of the characteristics of Archean

Downloaded from https://academic.oup.com/petrology/article-abstract/18/2/319/1565696 by University of California, San Diego Library user on 28 March 2019

komatiites are also present in younger terranes. To consider four examples: peridotite sills and magnesian basalts have been described by Wilson *et al.* (1969) and Schwartz & Fujiwara (1975) in the Proterozoic Cape Smith–Wakeham Bay (Ungava) belt of northern Quebec. The latter authors describe skeletal textures and conclude that the rocks are komatiites. Stephenson (1974) presents analyses from the Thompson, Manitoba mobile belt (presumed to incorporate Proterozoic rocks) and Peredery (personal communication) has recognized spinifex textures in some of these rocks. Gale (1973) suggests on the

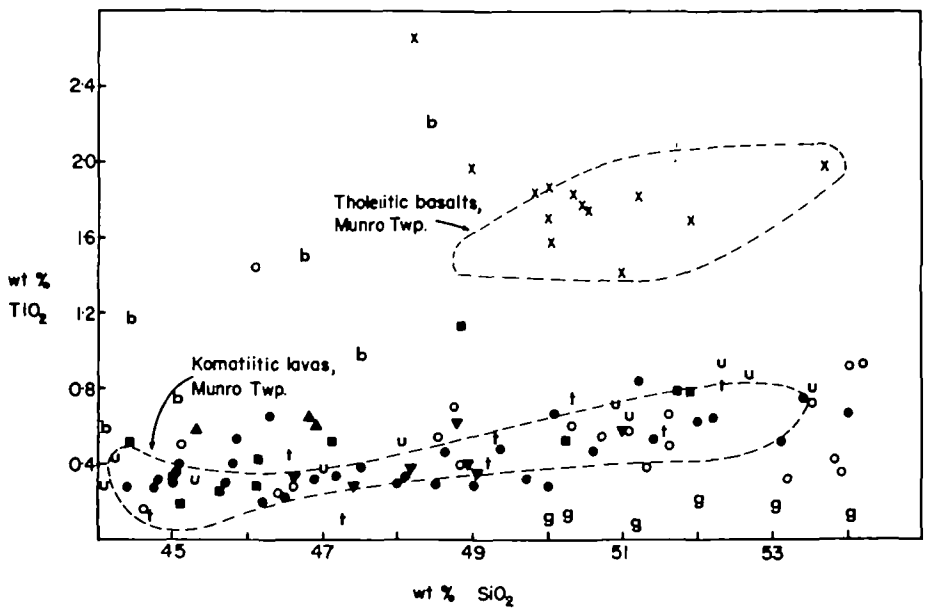

FIG. 29. TiO_2 *vs.* SiO_2 for komatiites and tholeiites. Legend as in Fig. 27.

basis of chemical data that aphanitic mafic lavas in the lower Palaeozoic Rambler Group of Newfoundland are komatiitic and Clark (1970) described MgO-rich basaltic rocks of Tertiary age from Baffin Island and West Greenland.

In Figs. 27 and 28, analyses of these rocks are plotted in FeO*/(FeO*+MgO) *vs.* Al_2O_3 and SiO_2 *vs.* TiO_2 diagrams. The Thompson and Ungava rocks are very similar to the komatiites of Munro Township. Taken in conjunction with the reported presence of spinifex texture, these data are firm evidence of the komatiitic nature of these rocks. Gale's (1973) Newfoundland rocks also have komatiitic characteristics, with very low TiO_2 contents. The Baffin Bay rocks, on the other hand, have high TiO_2 contents similar to those of Archean tholeiites (cf. Williams, 1972) and probably are not komatiites.

SUMMARY AND CONCLUSIONS

A study of the field, petrographic, and chemical characteristics of mafic and

Downloaded from https://academic.oup.com/petrology/article-abstract/18/2/319/1565696 by University of California, San Diego Library user on 28 March 2019

ultramafic volcanic and hypabyssal rocks of Munro Township, and comparisons of these rocks with others of similar type from other areas leads to the following conclusions:

1. All rocks in such areas fall into one of two magmatic associations, the komatiitic and tholeiitic associations. Included in each association are (a) thin flows of relatively uniform composition, (b) much thicker flows that are differentiated from peridotite at the base to gabbro near the top, and (c) simple or differentiated hypabyssal intrusions.

2. The komatiitic association contains rocks ranging from peridotitic to andesitic composition. Three types are recognized: peridotitic, pyroxenitic, and basaltic komatiites. These are distinguished by field, petrographic, and chemical criteria, and the limits of each category is defined precisely on the basis of MgO contents in H_2O-free analyses. Peridotitic komatiites have ultramafic compositions. The most ultramafic types are cumulates that form the basal parts of flows and sills, but slightly less mafic examples represent silicate liquids and commonly occur as spinifex-textured upper parts of flows. Peridotitic komatiites also form the flowtops and chilled margins of thick, layered flows and sills. Less mafic types, the pyroxenitic and basaltic komatiites, occur as flows with more normal dimensions and characteristics, and textures ranging from fine or medium-grained equigranular, to glassy, porphyritic or clinopyroxene spinifex.

3. The compositional range of tholeiitic rocks is smaller. The most mafic varieties are cumulate peridotites and pyroxenites of layered flows and sills; the most mafic rocks representing liquid compositions are picritic tops of layered flows. Lava flows and fragmental units with normal dimensions have basaltic or less mafic compositions. All tholeiites in Munro Township have high FeO^* and TiO_2 contents.

4. The most important characteristics of komatiites are the highly ultramafic compositions of many noncumulate rocks, spinifex texture, and the chemical features $FeO^*/(FeO^*+MgO)$ at a given Al_2O_3 content and TiO_2 content at a given MgO or SiO_2 value, both of which are lower in komatiites than in associated tholeiites.

5. Komatiitic rocks form a magma series of similar status to the tholeiitic or alkaline series. That all rocks called komatiites are genetically related is indicated by:

(*a*) the continuum of all chemical parameters, from the least mafic to the most ultramafic types;

(*b*) the presence in individual differentiated flows and sills of rocks ranging from ultramafic to mafic compositions;

(*c*) the indicated existence of silicate liquids of peridotitic komatiite composition, from which all other types of komatiite can be derived by crystal fractionation or accumulation.

Downloaded from https://academic.oup.com/petrology/article-abstract/18/2/319/1565696 by University of California, San Diego Library user on 28 March 2019

Other factors show that the komatiitic series is distinct from other better-known magma series:

(*a*) the features listed in Table 8 that distinguish between komatiites and associated tholeiites;

(*b*) the parameters illustrated in Fig. 22 that distinguish komatiites from rocks of the alkaline and calc-alkaline series;

(*c*) the relatively restricted stratigraphic and temporal distribution of komatiites, which are abundant only in the lowermost parts of volcanic-sedimentary cycles of Precambrian terranes.

6. Using the preceding points as a basis, it is possible to re-define the term komatiite. As is the case with other groups of rocks such as the tholeiites or calc-alkaline rocks, it is difficult to specify distinguishing characteristics of a single rock type such as a peridotitic komatiite; a more practical method is to treat the rocks as members of a series and to define the characteristics of the series as a whole. Thus we define the komatiitic series as follows:

(*a*) It comprises noncumulate rocks ranging in composition from peridotite ($\approx$30 per cent MgO, 44 per cent SiO_2) to basalt (8 per cent MgO, 52 per cent SiO_2) or andesite (12 per cent MgO, 56 per cent SiO_2), and cumulate rocks ranging from peridotite (up to 40 per cent MgO) to mafic gabbro ($\approx$12 per cent MgO). The compositions of the noncumulate rocks closely resemble the compositions of the silicate liquids from which they form.

(*b*) The series contains lavas that exhibit unusual textures and volcanic structures such as spinifex texture and polyhedral jointing.

(*c*) All members of the series have low $FeO^*/(FeO^*+MgO)$ ratios, low TiO_2 contents, and high MgO, NiO, and Cr_2O_3 content, and some, but not all, have high CaO/Al_2O_3 ratios.

ACKNOWLEDGMENTS

The first-named author did the research reported in this paper as a Ph.D. thesis project at the University of Toronto. The assistance of staff and technicians at the university, support during field work by Falconbridge Nickel Mines Ltd., and the receipt of a National Research Council of Canada Graduate Scholarship is acknowledged. Special thanks are due to Miss Elvira Gasparrini who is responsible for making the majority of the electron microprobe analyses in the laboratory directed and supported by Dr. J. C. Rucklidge of the University of Toronto. The work also was supported by National Research Council of Canada Grant No. A4244 awarded to Prof. A. J. Naldrett.

We wish to thank Dr. T. N. Irvine, B. O. Mysen, C. H. Donaldson, R. W. Nesbitt, and Messrs. A. H. Green and D. Fisher for critical reviews of the manuscript; and Mr. F. Jurgeneit who drafted many of the figures, Mr. B. O'Donovan who did the photography, and Mrs. L. Stewart who typed the manuscript.

Downloaded from https://academic.oup.com/petrology/article-abstract/18/2/319/1565696 by University of California, San Diego Library user on 28 March 2019

REFERENCES

ANHAEUSSER, C. R., 1971. Cyclic volcanicity and sedimentation in the evolutionary development of Archean greenstone belts of shield areas. *Spec. Publs. Geol. Soc. Aust.* **3**, 57–70.

ARNDT, N. T., 1975. Ultramafic rocks of Munro Township and their volcanic setting. *Unpub. Ph.D. thesis, Univ. of Toronto.*

—— 1976*a*. Melting relations of ultramafic lavas (komatiites) at one atmosphere and high pressure. *Yb. Carnegie Instn. Wash.* **75**, 555–61.

—— 1976*b*. Ultramafic lavas in Munro Township; economic and tectonic implications. In STRONG, D. F. (Ed.), *Metallogeny and Plate Tectonics, Spec. Publs. Geol. Ass. Can.* **14**, 617–58.

—— 1977. Thick, layered peridotite–gabbro lava flows in Munro Township. *Can. J. Earth Sci.* (in press).

BARNES, R. G., LEWIS, J. D., & GEE, R. D., 1974. Archean ultramafic lavas from Mount Clifford. *Rept. Geol. Surv. West. Aust.* 1973, 59–70.

BHATTACHARJI, S., 1967. Scale model experiments on flowage differentiation in sills. In WYLLIE, P. J. (Ed.), *Ultramafic and Related Rocks*, John Wiley & Sons, Inc., New York, 69–70.

BICKLE, M. S., MARTIN, A., & NISBET, E. G., 1975. Basaltic and peridotitic komatiites and stromatolites above a basal unconformity in the Belingwe greenstone Belt, Rhodesia. *Earth planet Sci. Lett.* **27**, 155–62.

BOTTINGA, Y., & WEILL, D. F., 1972. The viscosity of magmatic silicate liquids: a model for calculation. *Am. J. Sci.* **272**, 438–75.

BROOKS, C., & HART, S. R., 1972. An extrusive basaltic komatiite from a Canadian Archean metavolcanic belt. *Can. J. Earth Sci.* **9**, 1250–3.

—— —— 1974. On the significance of komatiite. *Geology*, **2**, 107–10.

BRYAN, W. B., 1972. Morphology of quench crystals in submarine basalts. *J. Geophys. Res.* **77**, 5812–19.

CARMICHAEL, I. S. E., 1964. The mineralogy of Thingmuli, a Tertiary volcano in eastern Iceland. *Am. Miner.* **52**, 1815–41.

CLARK, D. B., 1970. Tertiary basalts of Baffin Bay: possible primary magma from the mantle. *Contr. Miner. Petrol.* **25**, 203–25.

DONALDSON, C. H., 1974. Olivine morphology in the Tertiary harrisites of Rhum and in some Archean spinifex rocks. *Bull. Geol. Soc. Am.* **85**, 1721–6.

ECKSTRAND, O. R., 1972. Ultramafic flows and nickel deposits in the Abitibi orogenic belt. *Rep. Geol. Surv. Can.* **72–1A**, 75–82.

GALE, G. H., 1973. Palaeozoic basaltic komatiite and ocean-floor basalts from northeastern Newfoundland. *Earth planet. Sci. Lett.* **18**, 22–8.

GÉLINAS, L., & BROOKS, C., 1974. Archean quench-texture tholeiites. *Can. J. Earth Sci.* **11**, 324–40.

GEMUTS, I., & THERON, A., 1975. The stratigraphy and mineralization of the Archean between Norseman and Coolgardie, Western Australia. In *Ore Deposits of Australia and Papua–New Guinea; Monogr. Aust. Inst. Min. & Met.* **5**. 66–74.

GOODWIN, A. M., 1968. Evolution of the Canadian Shield. *Proc. Geol. Ass. Can.* **19**, 1–14.

—— 1973. Petrochemical trends in Archean volcanic assemblages, Abitibi Belt, Ontario and Quebec, Canada. *Abstr. with Programs (Geol. Soc. Am.)*, **5**, 641–2 (abstr.).

—— 1976. Archean volcanism in the Timmins–Kirland Lake-Noranda region of Ontario and Quebec. *Geol. Surv. Pap. Can.* (in press).

—— & RIDLER, R. H., 1969. The Abitibi orogenic belt. In BAYER, A. J. (Ed.), *Symposium on Basins and Geosynclines of the Canadian Shield, Geol. Surv. Pap. Can.* **28**, 70–40.

GREEN, D. H., NICHOLLS, I. A., VILJOEN, M. J., & VILJOEN, R. P., 1975. Experimental demonstration of the existence of peridotitic liquids in earliest Archean magmatism. *Geology*, **3**, 11–15.

HALLBERG, J. A., 1972. Geochemistry of Archean volcanic belts in the Eastern Goldfields Region of Western Australia. *J. Petrology*, **13**, 45–56.

IRVINE, T. N., 1970. Muskox Intrusion and Coppermine River Lavas, Northwest Territories, Canada. I. Olivine–pyroxene–plagioclase relations. *Spec. Publs. Geol. Soc. S. Afr.* **1**, 441–76.

JOLLY, W. T., 1974. Regional metamorphic zonation as an aid in study of Archean terranes; Abitibi region, Ontario. *Can. Miner.* **12**, 499–508.

—— 1975. Subdivision of Archean lavas of the Abitibi area, Canada, from Fe–Mg–Ni–Cr relations. *Earth planet. Sci. Lett.* **27**, 200–10.

KRETSCHMAR, U., & KRETSCHMAR, D., 1975. Geology and ultramafic flows of the Malartic Group, N.W. Quebec. *Abstr. with Program (Geol. Soc. Am., North-central Sect.)*, **7**, 801 (Abstr.).

KROGH, T. E., & DAVIS, G. L., 1971. Zircon U–Pb age of Archean metavolcanic rocks in the Canadian Shield. *Yb. Carnegie Instn. Wash.* **70**, 241–2.

Downloaded from https://academic.oup.com/petrology/article-abstract/18/2/319/1565696 by University of California, San Diego Library user on 28 March 2019

KUNO, H., 1966. Lateral variations of basalt magma type across continental margins and island arcs. *Bull. volcan.* **29**, 195–222.

KUSHIRO, I., 1969. The system forsterite–diopside–silica with and without water at high pressures. *Am. J. Sci., Schairer Vol.* **267A**, 269–94.

LEWIS, J. D., & WILLIAMS, I. R., 1973. The petrology of an ultramafic lava near Murphy Well, Eastern Goldfields, Western Australia. *Rep. Geol. Surv. West. Aust.* 1972, 60–8.

LOFGREN, G., 1974. An experimental study of plagioclase crystal morphology: isothermal crystallization. *Am. J. Sci.* **274**, 243–73.

—— DONALDSON, C. H., WILLIAMS, R. J., MULLINS, O., JR., & USSELMAN, T. M., 1974. Experimentally reproduced textures and mineral chemistry of Apollo 15 quartz normative basalts. *Proc. Fifth Lunar Sci. Conf., Geochim. cosmochim. Acta*, **I**, 549–68.

MACRAE, N. D., 1969. Ultramafic intrusions of the Abitibi area, Ontario. *Can. J. Earth Sci.* **6**, 281–303.

MCCALL, G. J. H., 1971. Some ultrabasic and basic igneous rock occurrences in the Archean of Western Australia. *Spec. Publ. Geol. Soc. Aust.* **3**, 429–42.

MEYER, H. O. A., 1975. Chromium and the genesis of diamond. *Geochim. cosmochim. Acta*, **39**, 929–36.

—— & GOODWIN, A. M., 1977. Volcanic rocks of the Blake River Group, Abitibi Greenstone Belt, and their sulfur content. *Can. J. Earth Sci.* (in press).

NALDRETT, A. J., & MASON, G. D., 1968. Contrasting Archean ultramafic igneous bodies in Dundonald and Clergue Townships, Ontario. *Can. J. Earth Sci.* **5**, 111–43.

—— & TURNER, A. R., 1977. The geology and petrogenesis of a greenstone belt and related nickel sulfide mineralization. *Precambrian Research* (in press).

NESBITT, R. W., 1971. Skeletal crystal forms in the ultramafic rocks of the Yilgarn block, Western Australia: Evidence for an Archean ultramafic liquid. *Spec. Publs. Geol. Soc. Aust.* **3**, 331–48.

—— & SUN, S. S., 1976. Geochemistry of Archean spinifex-textured peridotites and magnesian and low-magnesian tholeiites. *Earth planet Sci. Lett.* **31**, 433–53.

NOCKOLDS, S. R., & ALLEN, R., 1956. The geochemistry of some igneous rock series. *Geochim. cosmochim. Acta*, **4**, 105–42.

NORRISH, K., & CHAPPEL, B. W., 1967. X-ray fluorescence spectrography. In ZUSSMAN, J. (Ed.), *Physical Methods in Determinative Mineralogy*, 161–214.

PEARCE, T. H., & BIRKETT, T., 1974. Archean metavolcanic rocks from Thackeray Township, Ontario. *Can. Miner.* **12**, 509–19.

PYKE, D. R., & JENSEN, L. S., 1976. Preliminary stratigraphic interpretations of the Timmins–Kirkland Lake area, Ontario. *Program with Abstr. (Geol. Ass. Can.)*, **1**, 71 (Abstr.).

—— NALDRETT, A. J., & ECKSTRAND, A. R., 1973. Archean ultramafic flows in Munro Township, Ontario. *Bull. Geol. Soc. Am.* **84**, 955–78.

RUCKLIDGE, J. C., & GASPARRINI, E. L., 1969. A computer program for processing electron microprobe analytical data. *Dept. Geol., Univ. Toronto.*

SATTERLY, J., 1949. Geology of Garison Township. *Ontario Dept. Mines*, **63**, pt. 4.

—— 1951. Geology of Munro Township. *Ontario Dept. Mines*, **60**, pt. 8.

—— 1952. Geology of McCool Township. *Ontario Dept. Mines*, **61**, pt. 5.

—— & ARMSTRONG, H. S., 1947. Geology of Beatty Township. *Ontario Dept. Mines*, **56**, pt. 7.

SCHAU, M., 1975. Meta-komatiites in a stable Archean environment. *Abstr. with Programs (Geol. Soc. Am., North-central Sect.)*, **7**, 849 (Abstr.).

SCHWARZ, E. J., & FUJIWARA, Y., 1975. Circum-Ungava Fold Belt: Komatiitic basalts from the east coast of Hudson Bay. *Abstr. with Programs (Geol. Soc. Am., North-Central Sect.)*, **7**, 852 (Abstr.).

SHIMA, H., & NALDRETT, A. J., 1975. Solubility of sulfur in an ultramafic melt and the relevance of the system Fe–S–O. *Econ. Geol.* **70**, 960–7.

STEPHENSON, J. F., 1974. Geology of the Ospwagan Lake (East Half) area. *Manitoba Mines Branch, Publ.* **74–1**.

VILJOEN, M. J., & VILJOEN, R. P., 1969*a*. The geology and geochemistry of the lower ultramafic unit of the Onverwacht Group and a proposed new class of igneous rock. *Upper Mantle Project. Spec. Publs. Geol. Soc. S. Afr.* **2**, 221–44.

—— —— 1969*b*. Evidence for the existence of a mobile intrusive peridotite magma from the Komati Formation of the Onverwacht Group. *Upper Mantle Project. Spec. Publs. Geol. Soc. S. Afr.* **2**, 87–112.

—— —— 1969*c*. The geological and geochemical significance of the upper formations of the Onverwacht Group. *Upper Mantle Project. Spec. Publs. Geol. Soc. S. Afr.* **2**, 113–51.

VISWANATHAN, S., 1974. Basaltic komatiite occurrences in the Kolar gold field of India. *Geol. Mag.* **111**, 353–4.

Downloaded from https://academic.oup.com/petrology/article-abstract/18/2/319/1565696 by University of California, San Diego Library user on 28 March 2019

WALKER, D., KIRKPATRICK, R. J., LONGHI, J., & HAYS, J. F., 1976. Crystallization history of lunar picrite basalt 12002: Phase equilibria and cooling-rate studies. *Bull. Geol. Soc. Am.* **87**, 646–56.

WATKINS, N. D., GUNN, B. M., & COY-YLL, R., 1970. Major and trace element variations during the initial cooling of an Icelandic lava. *Am. J. Sci.* **268**, 24–49.

WILLIAMS, D. A. C., 1972. Archean ultramafic, mafic, and associated rocks, Mt. Monger, Western Australia. *J. Geol. Soc. Aust.* **19**, 163–88.

WILSON, H. D. B., KILBURN, L. C., GRAHAM, A. R., & RAMLAL, K., 1969. Geochemistry of some Canadian nickeliferous ultrabasic intrusions. *Monogr. Econ. Geol.* **4**, 294–309.

Downloaded from https://academic.oup.com/petrology/article-abstract/18/2/319/1565696 by University of California, San Diego Library user on 28 March 2019